

GOVT. DOC.

3.N21/516/2295

NATIONAL ADVISORY COMMITTEE FOR AERONAUTICS

TECHNICAL NOTE 2295

CHORDWISE AND COMPRESSIBILITY CORRECTIONS
TO SLENDER-WING THEORY

By Harvard Lomax and Loma Sluder

Ames Aeronautical Laboratory
Moffett Field, Calif.



February 1951

BUSINESS, SCIENCE
& TECHNOLOGY DEPT.

CONN. STATE LIBRARY

FEB 19 1951

ERRATA

→ NACA TN 2295

CHORDWISE AND COMPRESSIBILITY CORRECTIONS
TO SLENDER-WING THEORY

By Harvard Lomax and Loma Sluder

February 1951

Page 43, figure 5(b): The ordinate scale for $x_{c.p.}/c_o$ is in error and should be changed from 0, .4, .8, to .1, .5, .9.

NATIONAL ADVISORY COMMITTEE FOR AERONAUTICS

TECHNICAL NOTE 2295

CHORDWISE AND COMPRESSIBILITY CORRECTIONS

TO SLENDER-WING THEORY

By Harvard Lomax and Loma Sluder

SUMMARY

Corrections to slender-wing theory are obtained by assuming a spanwise distribution of loading and determining the chordwise variation which satisfies the appropriate integral equation. Such integral equations are set up in terms of the given vertical induced velocity on the center line or, depending on the type of wing plan form, its average value across the span at a given chord station. The chordwise distribution is then obtained by solving these integral equations. Results are shown for flat-plate, rectangular, and triangular wings.

INTRODUCTION

The calculation of loading on three-dimensional lifting surfaces is a fundamental problem in aerodynamic research. The complexity of the problem has lead to the development of certain simplified theories by means of which the loading on special types of plan forms can be estimated quickly. The amount of error which these estimates contain is of considerable interest, as are methods which will tend to correct such errors without undue labor.

Slender-wing theory applies to one such simplified body of analysis. There are two basic assumptions of this theory: one, the angle of attack is small enough so that the vortex sheet does not separate from the wing and the boundary conditions for the wing can be projected onto a horizontal plane parallel to the direction of the free stream; and the other, that either the chordwise gradient of velocity is small enough or the free-stream Mach number is close enough to unity that the linearized partial differential equation which governs the fluid flow becomes Laplace's equation in a plane transverse to the free-stream direction. References 1 through 5 are examples of recent papers developing slender-wing theory.

An indication of the magnitude of the error which is introduced by the use of such a theory comes, in the subsonic case, by observing that solutions so obtained violate the Kutta condition at the trailing edge. Proper inclusion of the chordwise and compressibility effects must result in solutions which satisfy the Kutta condition and make the loading fall to zero at the trailing edge. It is the purpose of this report to study such modifications.

The corrections due to the chordwise and compressibility effects are obtained in the following manner: First, an integral equation involving elementary horseshoe vortices is set up; second, this integral equation is solved under the assumption that the chordwise gradients are small or that the free-stream Mach number is unity; and finally, the integral equation is reinspected, this time with the spanwise lift distribution fixed at the shape just obtained and with the chordwise variation as the unknown and the Mach number terms included.

Results are presented and discussed both for triangular and rectangular, flat-plate plan forms in both subsonic and supersonic flow.

LIST OF IMPORTANT SYMBOLS

- a_0 velocity of sound in the free stream
- A aspect ratio $\left(\frac{b^2}{S} \right)$
- A_r reduced aspect ratio ($A_r = \beta A$)
- b span of wing measured normal to plane of symmetry
- c_0 root chord of wing
- C_L lift coefficient $\left(\frac{\text{lift}}{qS} \right)$
- C_m pitching-moment coefficient $\left(\frac{\text{pitching moment}}{qSc_0} \right)$
- E complete elliptic integral of the second kind with modulus k
- $$\left(E = \int_0^1 \sqrt{\frac{1-k^2t^2}{1-t^2}} dt \right)$$
- $E(t,k)$ incomplete elliptic integral of the second kind with argument t and modulus k $\left[E(t,k) = \int_0^t \sqrt{\frac{1-k^2t^2}{1-t^2}} dt \right]$

$F(t,k)$ incomplete elliptic integral of the first kind with argument t

and modulus k $\left[F(t,k) = \int_0^t \frac{dt}{\sqrt{(1-t^2)(1-k^2t^2)}} \right]$

K complete elliptic integral of the first kind with modulus k

$\left[K = \int_0^1 \frac{dt}{\sqrt{(1-t^2)(1-k^2t^2)}} \right]$

m for triangular wing, slope of leading edge relative to plane of symmetry

M_o free-stream Mach number $\left(\frac{V_o}{a_o} \right)$

p static pressure

Δp $p_l - p_u$

q free-stream dynamic pressure $\left(\frac{1}{2} \rho_o V_o^2 \right)$

s semispan of rectangular wing

S area of wing

u perturbation velocity component in the direction of the x axis

Δu $u_u - u_l$

V_o free-stream velocity

w perturbation velocity component in the direction of the z axis

w_o $-V_o \alpha$

x,y,z Cartesian coordinates of an arbitrary point

x_1,y_1 Cartesian coordinates of source or doublet position

x_o x/c_o

α angle of attack

β $\sqrt{|1-M_o^2|}$

θ_o βm

ρ_0	density in free stream
σ, σ_p	doublet weighting factors
φ	perturbation velocity potential
$\Delta\varphi$	$\varphi_u - \varphi_l$

Subscripts

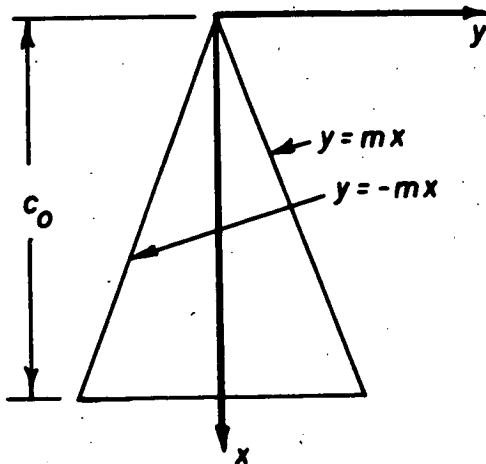
l	conditions on lower surface of wing (at $z = 0^-$)
u	conditions on upper surface of wing (at $z = 0^+$)

THE INTEGRAL EQUATIONS

Subsonic

Triangular plan form.— A general solution of Laplace's equation which is suited to problems in linearized subsonic wing theory (given e.g., in reference 6) is that which relates a velocity potential or perturbation velocity to the value of its jump across a given surface. For a lifting triangular wing as shown in the sketch this can be written

$$u = \frac{z\beta^2}{4\pi} \int_0^{c_0} dx_1 \int_{-mx_1}^{mx_1} \frac{\Delta u \, dy_1}{[(x-x_1)^2 + \beta^2(y-y_1)^2 + \beta^2 z^2]^{3/2}} \quad (1)$$



where $\beta = \sqrt{1-M_0^2}$, u is the perturbation velocity parallel to the x axis and Δu is the jump in u over the wing plan form. In linearized theory this jump can be related to the loading coefficient $\Delta p/q$ by the equation

$$\Delta u = \frac{V_0}{2} \left(\frac{\Delta p}{q} \right) \quad (2)$$

Further, the velocity potential φ can be found by the relation

$$\varphi = \int_{-\infty}^x u \, dx$$

Operating on equation (1) in this manner and interchanging the order of integration gives

$$\phi = \frac{zV_0}{8\pi} \int_0^{c_0} dx_1 \int_{-mx_1}^{mx_1} \frac{\left(\frac{\Delta p}{q}\right) dy_1}{[(y-y_1)^2 + z^2]} \left[1 + \frac{x-x_1}{\sqrt{(x-x_1)^2 + \beta^2 z^2 + \beta^2 (y-y_1)^2}} \right] \quad (3)$$

which represents, physically, a distribution of elementary horseshoe vortices.

The effect of compressibility in a linearized study of lifting-surface theory can only enter through the use of β . Setting

$$\sigma = 1 + \frac{(x-x_1)}{\sqrt{(x-x_1)^2 + \beta^2 (y-y_1)^2 + \beta^2 z^2}} \quad (4)$$

it is seen that σ is the only term in equation (3) which contains β . This term has an interesting interpretation in the light of the study which has been made at sonic speeds. At $M_0 = 1$ (i.e., $\beta = 0$), σ has either the value 2 or 0, depending on whether x_1 is less or greater than x . Hence, equation (3) becomes

$$\phi = \frac{zV_0}{4\pi} \int_0^x dx_1 \int_{-mx_1}^{mx_1} \frac{\left(\frac{\Delta p}{q}\right) dy_1}{(y-y_1)^2 + z^2} \quad (5)$$

Now reversing the order of integration and using the definition implied by equation (2), namely,

$$\frac{\Delta p}{q} = \frac{2}{V_0} \frac{\partial \Delta \phi}{\partial x_1}$$

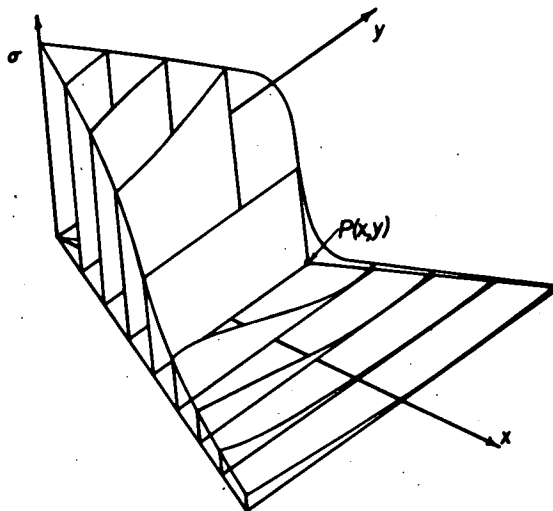
gives finally

$$\phi = \frac{z}{2\pi} \int_{-mx}^{mx} \frac{\Delta \phi dy_1}{(y-y_1)^2 + z^2} \quad (6)$$

Equation (6) has been studied in reference 5 as the fundamental equation for slender wings or wings flying at near sonic speeds. It is an equation which gives the solution for the velocity potential in a three-dimensional flow in terms of two-dimensional doublets, the two dimensions being at right angles to the free-stream direction. A solution of such a nature is immediately implied by the physical character of both sonic wing theory, in which the Mach cone has degenerated to a Mach plane, and slender-wing theory, in which the wing is so slender that the chordwise

gradient of velocities can be neglected compared to the vertical and lateral gradients.

By comparison of equation (5) with equation (3), it is seen that the term σ can be interpreted as a factor which corrects the slender-wing-theory results as given by equation (5) for the effects of chord-wise gradients in velocity and compressibility. By consideration of the effect at one point of the distribution of doublets over the wing, this correction can be visualized as a reweighting of the two-dimensional doublets according to their position relative to the point. The sketch indicates the variation of σ across the span at various chord stations for $\beta = 0.6$. Observe that the doublets ahead of the point at which the potential is to be determined are still weighted far more heavily than those behind the point. The effect of considering β different from zero, however, is to reduce the extreme difference in weight occasioned at $\beta = 0$ so that the doublets behind a given point do have some effect on the induced velocities there, and the doublets ahead of a point induce a somewhat smaller disturbance than before. Since the strength of these weighted two-dimensional doublets is given by the magnitude of the three-dimensional loading, their strength is zero everywhere off the wing plan form including the area behind the wing occupied by the vortex wake.



Two different methods for the further reduction of equation (3) will be considered. The first method involves finding the vertical induced velocity for points along the x axis, while the second involves finding the average vertical induced velocity along the span at a given chord station. The first method must be discarded for triangular wings because of difficulties around the apex; the second, however, proves to be quite satisfactory. The simplification obtained by considering the vertical induced velocity for points along the x axis will be considered later in connection with the rectangular wing.

Since it is easier to consider first the averaging process, the operator

$$\lim_{z \rightarrow 0} \frac{1}{2\pi x} \frac{\partial}{\partial z} \int_{-mx}^{mx} dy$$

is applied to the weighted doublets, $\sigma z / [(y-y_1)^2 + z^2]$, of equation (3) with the result that

$$\bar{w} = -\frac{V_0}{8\pi} \int_0^{c_0} dx_1 \int_{-mx_1}^{mx_1} dy_1 \frac{\left(\frac{\Delta p}{q}\right)}{m^2 x^2 - y_1^2} - \frac{V_0}{8\pi} \int_0^{c_0} dx_1 \int_{-mx_1}^{mx_1} \frac{\left(\frac{\Delta p}{q}\right)}{2mx(x-x_1)} \left[\frac{\sqrt{(x-x_1)^2 + \beta^2(mx-y_1)^2}}{mx-y_1} + \frac{\sqrt{(x-x_1)^2 + \beta^2(mx+y_1)^2}}{mx+y_1} \right] dy_1 \quad (7)$$

where \bar{w} is the average value of the vertical induced velocity along a given span.

The solution for $\Delta p/q$ obtained from slender-wing theory can be written¹

$$\frac{\Delta p}{q} = -\frac{4w_0 m^2 x_1}{V_0 \sqrt{m^2 x_1^2 - y_1^2}} f_1\left(\frac{x_1}{c_0}\right) \quad (8)$$

where in that theory $f_1(x_1/c_0) = 1$. If the value of $\Delta p/q$ given by equation (8) is placed in equation (7), the resulting integral equation can be written in a simplified form if it is noted that

$$I_1 = \int_{-mx_1}^{mx_1} \left[\frac{\sqrt{(x-x_1)^2 + \beta^2(mx-y_1)^2}}{mx-y_1} + \frac{\sqrt{(x-x_1)^2 + \beta^2(mx+y_1)^2}}{mx+y_1} \right] \frac{\frac{1}{2} m dy_1}{\sqrt{m^2 x_1^2 - y_1^2}} \\ = m \int_{m(x-x_1)}^{m(x+x_1)} \frac{\sqrt{(x-x_1)^2 + \beta^2 \eta^2} d\eta}{\eta \sqrt{-m^2(x^2 - x_1^2) + 2\eta mx - \eta^2}} \quad (9)$$

where for the first term in the brackets the transformation $\eta = mx - y_1$ was used and for the second the transformation $\eta = mx + y_1$. Hence, equation (7) finally reduces to the following

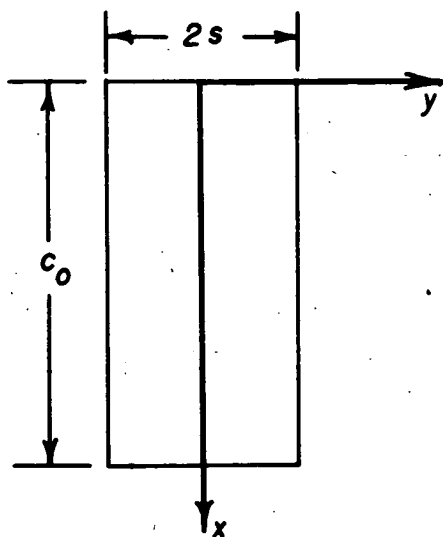
$$\bar{w} = \frac{w_0}{2\pi x} \left[\int_0^x \frac{\pi x_1 f_1\left(\frac{x_1}{c_0}\right)}{\sqrt{x^2 - x_1^2}} dx_1 + \int_0^{c_0} \frac{x_1 I_1 f_1\left(\frac{x_1}{c_0}\right)}{(x-x_1)} dx_1 \right] \quad (10)$$

The solution of equation (10) will be discussed in a later section devoted to triangular wings.

¹This solution follows from an analysis of equation (6). See reference 5.

Rectangular plan form.— If the plan form of the wing is rectangular as shown in the sketch, then equation (3) is modified slightly to the form

$$\phi = \frac{zV_0}{8\pi} \int_0^{c_0} dx_1 \int_{-s}^s \frac{\sigma \frac{\Delta p}{q} dy_1}{(y-y_1)^2 + z^2} \quad (11)$$



It is possible in this case to study the vertical induced velocity for points along the x axis; that is, to find $\partial\phi/\partial z$ by equation (11) and then set both y and z equal to zero. In order to do this a special notation must be employed. Thus, if the indefinite integral of $f(y)/y^2$ can be written (where $f(y)$ is bounded at $y = 0$)

$$\int \frac{f(y)}{y^2} dy = -J(y) + C$$

Then, by definition,

$$\int \frac{f(y)}{y^2} dy \equiv J(s) - J(-s) \quad (12)$$

By means of this definition it can be shown that (reference 7)

$$w = \frac{V_0}{8\pi} \int_0^{c_0} dx_1 \int_{-s}^s dy_1 \left(\frac{\Delta p}{q} \right) \frac{1}{y_1^2} \left[1 + \frac{x-x_1}{\sqrt{(x-x_1)^2 + \beta^2 y_1^2}} \right] \quad (13)$$

and if²

$$\frac{\Delta p}{q} = -4 \frac{w_0}{V_0 c_0} f_2 \left(\frac{x}{c_0} \right) \sqrt{s^2 - y^2} \quad (14)$$

²The solution for the rectangular wing in slender-wing theory is that the load be zero across every spanwise strip aft of the leading edge. To find the chordwise correction to such a theory, therefore, a spanwise distribution must be assumed. Since, however, slender-wing theory also requires an elliptical span loading for the boundary conditions of a rectangular wing to be satisfied, a reasonable choice is that given by equation (14).

Then, since integrating by parts gives

$$I_2 = - (x-x_1)^2 \int_{-s}^s \frac{dy_2}{y_1^2} \sqrt{\frac{s^2-y_1^2}{(x-x_1)^2+\beta^2 y_1^2}} = \int_{-s}^s \sqrt{\frac{(x-x_1)^2+\beta^2 y_1^2}{s^2-y_1^2}} dy_1 \quad (15)$$

equation (13) can be written

$$w = \frac{w_0}{2\pi c_0} \int_0^{c_0} \left(\pi + \frac{I_2}{x-x_1} \right) f_2 \left(\frac{x_1}{c_0} \right) dx_1 \quad (16)$$

This integral equation has been derived previously by K. Wieghardt (reference 8) with regard to the rectangular-wing problem. The solution of equation (16) will be discussed in a later section devoted to rectangular wings.

Supersonic

Triangular plan form.— In passing from subsonic to supersonic theory, we pass from the elliptic to the hyperbolic partial differential equation and in particular from Laplace's equation to the wave equation. The solution which relates the perturbation velocity u at any point in the field to the loading on the wing can again be written in terms of an elementary horseshoe vortex distribution over the wing plan form. As in reference 9 this becomes

$$u = \frac{z}{2\pi} \frac{\partial}{\partial x} \iint_{\tau} \frac{(x-x_1) \Delta u \, dx_1 \, dy_1}{[(y-y_1)^2+z^2] \sqrt{(x-x_1)^2-\beta^2(y-y_1)^2-\beta^2 z^2}}$$

and since $u = \frac{\partial \phi}{\partial x}$ and $\frac{\Delta p}{q} = \frac{2\Delta u}{V_0}$,

$$\phi = \frac{V_0 z}{4\pi} \iint_{\tau} \frac{\frac{\Delta p}{q} \, dx_1 \, dy_1}{(y-y_1)^2+z^2} \left[\frac{x-x_1}{\sqrt{(x-x_1)^2-\beta^2(y-y_1)^2-\beta^2 z^2}} \right] \quad (17)$$

where τ is the area on the wing bounded by the edges and the trace of the Mach forecone from the point x, y, z . Again the effect of compressibility appears only in the term within the braces so that by defining

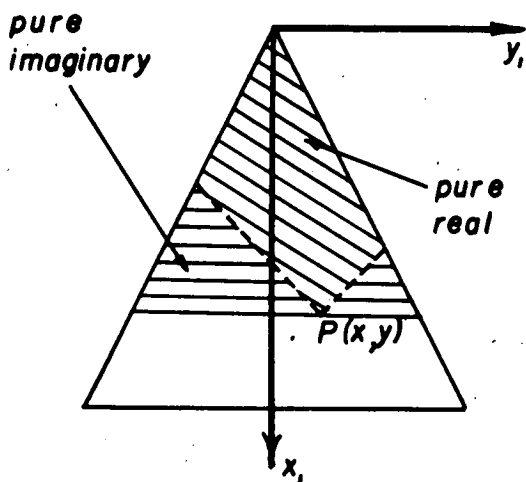
$$\sigma_p = \frac{x-x_1}{\sqrt{(x-x_1)^2-\beta^2(y-y_1)^2-\beta^2 z^2}} \quad (18)$$

σ_p contains all of the Mach number effects at supersonic speeds. At $M_0 = 1$, $\sigma_p = 1$, and since, by the definition of τ , $x_1 \leq x$, it follows that at sonic speeds equation (17) also reduces to equation (5). Hence, the doublet distributions represented by equations (17) and (3) are consistent at the speed of sound.

In order that an exact parallel can be provided with the subsonic solution to the triangular wing, the average vertical induced velocity for points along a given span is again considered. It can be shown (reference 7) that in the plane of the wing

$$w = -\frac{\beta V_0}{4} \frac{\Delta p}{q} + \frac{V_0}{4\pi} \text{R.P.} \int_0^x dx_1 \int_{-mx_1}^{mx_1} dy_1 \frac{(x-x_1) \frac{\Delta p}{q}}{(y-y_1)^2 \sqrt{(x-x_1)^2 - \beta^2(y-y_1)^2}} \quad (19)$$

where the order of integration must be indicated (i.e., the integration with respect to y_1 must be made first). The letters R.P. indicate the real part of the term is to be taken. Such a device can be used since the double integral must always be a pure real quantity in the area τ ($\Delta p/q$ is real everywhere on the plan form) and a pure imaginary quantity over the rest of the area indicated (see sketch). The average vertical induced velocity along the span may be obtained by applying to equation (19) the operator



$$\frac{1}{2mx} \int_{-mx}^{mx} dy$$

and since

$$\frac{\Delta p}{q} = -\frac{4w_0 m^2 x_1}{V_0 \sqrt{m^2 x_1^2 - y_1^2}} f_3(x_1) \quad (20)$$

equation (19) may be written in the form

$$\bar{w} = \frac{\pi \beta m w_0 f_3(x)}{2} +$$

$$\frac{w_0}{\pi x} \int_0^x \frac{x_1 I_3 f_3(x_1) dx_1}{x - x_1} \quad (21)$$

I_3 has a derivation similar to that used for equation (9) and can be expressed in the final form as

$$I_3 = m \text{ R.P. } \int_{m(x-x_1)}^{m(x+x_1)} \frac{\sqrt{(x-x_1)^2 - \beta^2 \eta^2} d\eta}{\eta \sqrt{[m(x_1+x)-\eta][m(x_1-x)+\eta]}} \quad (22)$$

It is possible to find an exact solution for $f_3(x)$ by means of equation (21), but the discussion of this analysis is reserved for a subsequent section.

Rectangular plan form.— Equation (19) can also be used in the case of a rectangular plan form by an appropriate change in limits; thus,

$$w = -\frac{\beta V_0 \frac{\Delta p}{q}}{4} + \frac{V_0}{4\pi} \text{ R.P. } \int_0^x dx_1 \int_{-s}^s dy_1 \frac{(x-x_1) \frac{\Delta p}{q}}{(y-y_1)^2 \sqrt{(x-x_1)^2 - \beta^2 (y-y_1)^2}} \quad (23)$$

where again it should be stressed that the order of integration cannot be reversed. The region of integration and position of the wing with reference to the axis is shown in the sketch. As in the case of the subsonic rectangular wing, the value of w will be obtained only along the x axis so that y in equation (23) can be set equal to zero. The loading will be assumed to have a form

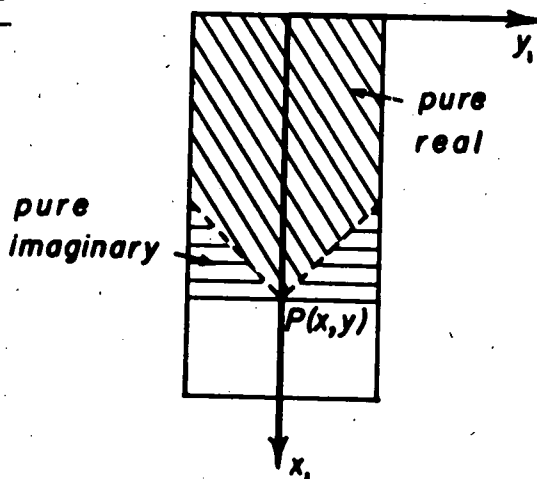
$$\frac{\Delta p}{q} = -4 \frac{w_0}{V_0 s \beta} f_4 \left(\frac{x}{s \beta} \right) \sqrt{s^2 - y^2} \quad (24)$$

which is similar to that used in the subsonic case except that the reference length is now the semispan instead of the chord. Such a difference is reasonable since in the supersonic case the position of the trailing edge cannot effect the loading on the wing.

Finally, therefore, when $y = 0$ equation (23) becomes

$$w = w_0 f_4 \left(\frac{x}{s \beta} \right) + \frac{w_0}{\pi s \beta} \int_0^x \frac{I_4 f_4 \left(\frac{x_1}{s \beta} \right)}{x-x_1} dx_1 \quad (25)$$

where I_4 is given by the equation



$$I_4 = \text{R.P.} \int_{-s}^s \sqrt{\frac{(x-x_1)^2 - \beta^2 y_1^2}{s^2 - y_1^2}} dy_1 \quad (26)$$

The solution to equation (25) is deferred to a subsequent section.

LOADING ON WINGS

The previous section was devoted to the development of the integral equations which are to be studied for the two types of plan forms in subsonic and supersonic flight. In order that this study can proceed in a natural manner, the arrangement of the presentation has been changed so that the plan form is the principal division and the speed is subsidiary.

Triangular Wings

Supersonic case.— The decision to solve for the loading on the supersonic, triangular, flat plate by analyzing equation (21) was not an obvious one since the exact solution of the linearized partial differential equation for this case has already been obtained. (See, e.g., references 10, 11, and 12.) Thus it is known before starting that the value of $f_3(x)$ in equation (21) must be $1/E$ where E is the complete elliptic integral of the second kind with modulus $\sqrt{1-m^2\beta^2}$. However, these solutions were obtained by an entirely different procedure so that by solving equation (21) and comparing the two results a check on the accuracy of the method is obtained. Furthermore, when the subsonic problem is analyzed the same general procedure will be followed and the results can then be accepted with greater confidence.

The first step in the solution of equation (21), in which \bar{w} has been set equal to w_0 since the wing is a flat plate, is to change variables by the transformation $\xi_1 = x_1/x$. This gives

$$1 = \frac{\pi\beta m}{2} f_3(x) + \frac{1}{\pi} \int_0^1 \frac{\xi_1 f_3(x\xi_1) d\xi_1}{1-\xi_1} I_3(\xi_1) \quad (27)$$

In the equation for I_3 , the transformation $m\eta_1 = \eta/x$ was used so that

$$I_3 = \int_{1-\xi_1}^{1+\xi_1} \frac{\sqrt{(1-\xi_1)^2 - \beta^2 m^2 \eta_1^2}}{\eta_1 \sqrt{(\xi_1 + 1 - \eta_1)(\xi_1 - 1 + \eta_1)}} d\eta_1$$

which is completely independent of x . The partial derivative of both sides of equation (27) with respect to x gives

$$f_3'(x) = - \frac{2}{\pi^2 \beta_m} \int_0^1 \frac{\xi_1^2 f_3'(x \xi_1) d\xi_1}{1 - \xi_1} I_3(\xi_1) \quad (28)$$

Equation (28) is a homogeneous linear integral equation. The solution to equation (28) is simply $f_3'(x) = 0$ or, what is equivalent, $f_3(x)$ equals a constant, $(f_3)_0$ say. By means of equation (27), this constant can be evaluated. Hence,

$$(f_3)_0 = \left[\frac{\pi \beta_m}{2} + \frac{1}{\pi} \int_0^1 \frac{\xi_1 I_3(\xi_1) d\xi_1}{1 - \xi_1} \right]^{-1} \quad (29)$$

which represents the solution to the problem. The integral I_3 was calculated analytically as in appendix A, and then the value of $(f_3)_0$, as given by equation (29), was determined by numerical integration. For $\beta_m = 0.8$ the result of this computation was 0.708; whereas the true value given by $1/E$ is 0.705.

Equation (27) can also be solved when the wing is slender with respect to the Mach cone by considering β_m to be small. Setting $\beta_m = 0$ yields

$$(I_3)_{\beta_m=0} = (1 - \xi_1) \int_{(1-\xi_1)}^{(1+\xi_1)} \frac{d\eta_1}{\eta_1 \sqrt{(\xi_1 + 1 - \eta_1)(\xi_1 - 1 + \eta_1)}}$$

and this is readily evaluated to give

$$(I_3)_{\beta_m=0} = \frac{\pi(1 - \xi_1)}{\sqrt{1 - \xi_1^2}} \quad (30)$$

The integral equation reduces to

$$1 = \int_0^1 \frac{\xi_1 f_3(x \xi_1) d\xi_1}{\sqrt{1 - \xi_1^2}}$$

which by a retransformation of variables $x_1 = x \xi_1$ becomes

$$x = \int_0^x \frac{x_1 f_3(x_1) dx_1}{\sqrt{x^2 - x_1^2}} \quad (31)$$

Equation (31) is a special form of Abel's integral equation, the unique inversion³ of which is, in this case, $f_3(x) = 1$. This is easily verified by direct substitution.

The simplicity of this result is not accidental, of course, since the value of $f_3(x)$ was originally introduced by equation (20) as a correction factor to the slender-wing-theory solution.

Subsonic case.— The study of the triangular wing presented in the preceding section was made first at arbitrary supersonic Mach numbers and then at a Mach number equal to 1. In keeping with this order of decreasing speed, the subsonic flat plate will be studied first at sonic speed and then for general subsonic Mach numbers.

An inspection of equations (9) and (22) is sufficient to show that $(I_1)_{\beta_m=0}$ is equal to $(I_3)_{\beta_m=0}$. Hence, equation (30) can be substituted into equation (10) and there results (since again \bar{w} is set equal to w_0)

$$1 = \frac{1}{2\pi x} \left[\int_0^x \frac{\pi x_1 f_1\left(\frac{x_1}{c_0}\right) dx_1}{\sqrt{x^2 - x_1^2}} + \int_0^x \frac{\pi x_1 f_1\left(\frac{x_1}{c_0}\right) dx_1}{\sqrt{x^2 - x_1^2}} \right]$$

and this reduces immediately to

$$x = \int_0^x \frac{x_1 f_1\left(\frac{x_1}{c_0}\right) dx_1}{\sqrt{x^2 - x_1^2}} \quad (32)$$

It is now obvious that equation (31), which was derived from supersonic wing theory, and equation (32), which was derived from subsonic wing theory, are identical. Clearly this establishes the continuity of the theory in passing from the supersonic to the subsonic regimes.

³If Abel's equation is written in the form

$$f(x) = \int_a^x \frac{u(\xi) d\xi}{\sqrt{x - \xi}}$$

its inversion is

$$u(z) = \frac{1}{\pi} \frac{d}{dz} \int_a^z \frac{f(x) dx}{\sqrt{z - x}}$$

The analysis for the general subsonic case leads eventually to the numerical solution of an integral equation. However, an idea of the qualitative form which this solution must assume can be gained by a rough preliminary analysis before resorting to the more tedious procedures necessary for a quantitative evaluation.

The evaluation of I_1 is given in appendix A, and a plot of $\frac{1}{2}I_1$ against x_1/x for $(\beta m)^2$ equal to 0, 0.05, 0.10, and 0.20 is shown in figure 1. Subtracting from I_1 its value at $\beta m = 0$, and denoting this difference by I_{11} , it follows that

$$I_{11} = \begin{cases} I_1 - \pi \sqrt{\frac{x-x_1}{x+x_1}} & x_1 \leq x \\ I_1 & x_1 \geq x \end{cases} \quad (33)$$

and equation (10) becomes

$$1 = \frac{1}{2\pi x} \left[\int_0^x \frac{2\pi x_1 f_1\left(\frac{x_1}{c_0}\right) dx_1}{\sqrt{x^2 - x_1^2}} + \int_0^{c_0} \frac{x_1 I_{11} f_1\left(\frac{x_1}{c_0}\right) dx_1}{x - x_1} \right] \quad (34)$$

As a rough approximation, since $I_{11}/2\pi$ is small and tends to zero as βm goes to zero, consider $\epsilon = I_{11}/2\pi$ to be a small constant which can be taken through the integral sign so that equation (34) becomes

$$x = \int_0^x \frac{x_1 f_1\left(\frac{x_1}{c_0}\right) dx_1}{\sqrt{x^2 - x_1^2}} + \epsilon \int_0^{c_0} \frac{x_1 f_1\left(\frac{x_1}{c_0}\right) dx_1}{x - x_1} \quad (35)$$

For ϵ equal to zero the solution to equation (35) is, of course, $f_1(x_0) \equiv 1$ as has already been discussed. For a small but finite value of ϵ , the second term will not have much effect on $f_1(x_0)$ near the center of the wing chord, but near the apex and trailing edge it becomes dominant since the value $f_1(x_0) = 1$ makes this term logarithmically infinite at these two extremes. Thus, the second term must certainly be reckoned with in finding the solution for $f_1(x_0)$ even though ϵ is small.

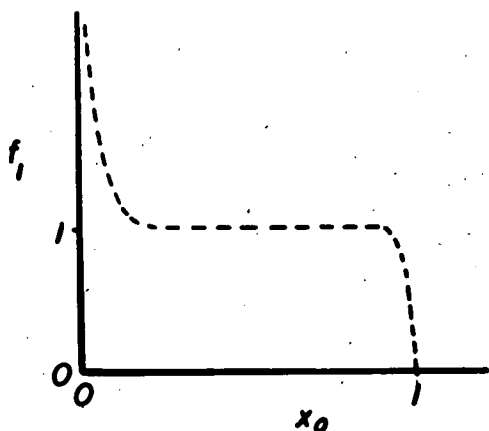
Now it is apparent that the right-hand term of equation (35) makes that expression a singular integral equation. Experience with the singular integral equation

$$f(y) = \int_0^1 \frac{g(y_1) dy_1}{y - y_1}$$

which arises in subsonic lifting-line theory and two-dimensional airfoil-section theory proves useful in the present problem. Thus, the solution to equation (35) is not unique unless the Kutta condition is specified at the trailing edge, and, furthermore, the value of $f_1(x_0)$ tends to infinity as x approaches the apex and to zero as x approaches the trailing edge.

One would, therefore, anticipate the shape of the solution for $f_1(x_0)$ to be something like that shown in the sketch. Such qualitative knowledge is useful in setting up the numerical procedure used for the

correct solution to equation (10). The presentation of this procedure appears in appendix B and the results of the analysis for A_r equal to 0, 0.90, 1.26, and 1.79 are given graphically by figure 2.



The figure shows that the shape of $f_1(x_0)$ which was sketched was fairly accurate. Further, the values in the figure indicate that the center of pressure shifts forward with increasing values of βm . A more comprehensive discussion of the integrated values of the loading will be given in a later section.

Rectangular Wings

The discussion of the triangular wing was divided according to the Mach number. The same division will be used for this section starting with the discussion of the results for supersonic speeds, then the results of both supersonic and subsonic theories at sonic speeds and finally a discussion of the subsonic development.

Supersonic case.— The solution of equation (25) will give the loading on a rectangular wing flying at a supersonic Mach number. The evaluation of the integral I_4 is carried out in appendix A where it is shown that I_4 can be expressed in terms of complete elliptic integrals of the first and second kinds. Having the expression for I_4 , a numerical solution may be obtained for $f_4(x/s\beta)$ when $w = w_0$, that is when the wing is flat. (See appendix B.) Figure 3 shows a plot of f_4 (a factor representative of the chord lift distribution) as a function of $x/s\beta$, the ratio of the distance back from the leading edge to the magnitude of the reduced semispan. The value of f_4 given by equation (25) can be checked

in the interval $0 \leq (x/s\beta) \leq 2$ because the exact solution to the complete linearized partial differential equation can be readily obtained there. The comparison is given in figure 3. The fairly rough agreement shown is not surprising since equation (25) is derived on the assumption that the spanwise distribution of load is elliptical at every chord station, and certainly this assumption is least accurate in the interval where the comparison with the exact results is made. The area under the exact and approximate curves in figure 3, between the initial value and that at which $f_4 = 0$, is nearly the same. (See the next section on Aerodynamic Characteristics.) The integrated value of f_4 as given by equation (25), therefore, should be sufficiently accurate for $x/s\beta > 2$.

As for the qualitative nature of the variation, figure 3 shows that the loading on a narrow rectangular wing flying at supersonic speeds falls linearly to zero, becomes negative, and then oscillates between negative and positive values; the amplitude of the oscillation being so heavily damped that after the third change in sign the magnitude is practically zero.

It should be noticed in studying the results of figure 3 that the entire resultant lift of the wing is concentrated in the interval $0 \leq (x/s\beta) \leq 2$. But as the Mach number approaches 1 this interval approaches zero, and the entire lift of the wing is carried in a strip along the leading edge.⁴ Such a solution violates, in the vicinity of the leading edge, the assumption on which the theory is based and should be considered only as a theoretical limit.

Results for the lift and pitching moment on the rectangular wing will be developed in a later section.

Subsonic case.— The study of the subsonic rectangular wing stems from equation (16). The first step in the analysis of the equation will be to consider its solution at $\beta s = 0$ and show that this is continuous with the supersonic results there.

The value of I_2 can be written (equation (15)) as

$$I_2 = \int_{-1}^1 \frac{\sqrt{(x-x_1)^2 + \beta^2 s^2 y^2}}{1-y^2} dy$$

and for $\beta s = 0$ this becomes

$$I_2 = \begin{cases} (x-x_1)\pi & x_1 \leq x \\ -(x-x_1)\pi & x_1 \geq x \end{cases}$$

⁴This result also follows by inspecting equation (25) for the values $\beta s = 0$.

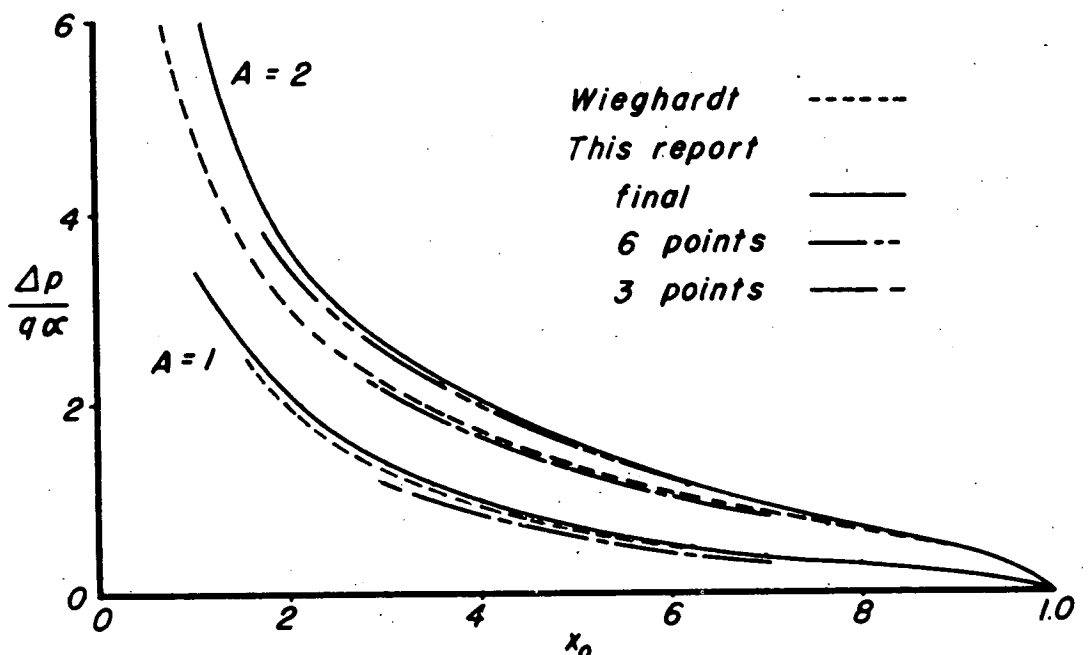
and hence equation (16) can be written

$$w = \frac{w_0}{c_0} \int_0^x f_2 \left(\frac{x_1}{c_0} \right) dx_1 \quad (36)$$

Equation (36) is identical with the form of the supersonic equation (25) at $\beta_s = 0$ so that once again the continuity of the subsonic and supersonic theories at the sonic speed range is established. Furthermore, equation (36) shows that if w/w_0 is constant then $f_2(x_0)$ must be zero everywhere except at points where it can be represented by a pulse the integral of which has a finite magnitude. From the supersonic discussion, it is clear that one such pulse exists and is located at the leading edge.

The evaluation of I_2 for $\beta_s > 0$ is given in appendix A. The numerical solution to equation (16), assuming the Kutta condition at the trailing edge, is given in appendix B for values of reduced aspect ratio A_r (defined as β times aspect ratio) equal to 0.33, 1.0, 1.5, and 2.0. For an aspect ratio equal to 2, these values correspond to Mach numbers of 0.986, 0.866, 0.662, and 0, respectively. The results of the computations are shown in figure 4 where the chordwise lift distribution factor $f_2(x_0)$ is plotted against x_0 for the various values of A_r . By comparison of figure 4 with figure 3, it can be seen that in the subsonic case the loading drops monotonically from infinity at the leading edge to zero at the trailing edge and does not oscillate in the after portion, as in the case of the supersonic wing.

When β equals one, these results can be compared with those obtained by Wieghardt and presented in reference 8. The sketch shows the comparison for two values of the aspect ratio. Curves are also



shown in the figure for the loading obtained by using the method given in the appendix of this report but by satisfying the integral equation at only six and three points. The latter curve is in better agreement with Wieghardt's result and, since Wieghardt (although using a different method involving Birnbaum functions) used only 4 points, this may account for the discrepancy between the final results of this report and those of Wieghardt.

AERODYNAMIC CHARACTERISTICS

The previous section presented solutions for the loading on triangular and rectangular wings flying at subsonic and supersonic speeds. This section will be devoted to the conversion of these loadings to expressions for lift and center of pressure.

Lift

By definition the lift coefficient can be written

$$C_L = \frac{1}{S} \iint_S \frac{\Delta p}{q} dx dy \quad (37)$$

and this will be evaluated for the various cases for which the loading coefficient has been obtained.

Supersonic triangular wing.— Since the exact linearized value for the loading on the triangular wing flying at supersonic speeds has been derived, the lift coefficient can be written in the form

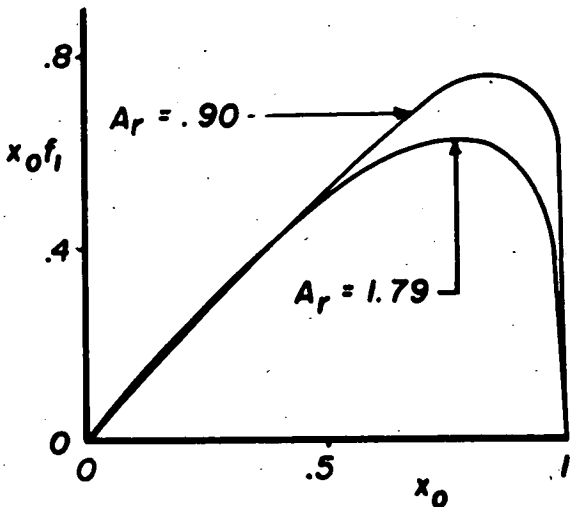
$$\frac{C_L}{\alpha A} = \frac{\pi}{2E} \quad (38)$$

where A is the aspect ratio and E is the elliptic integral of the second kind with modulus $k = \sqrt{1 - \beta^2 m^2}$.

Subsonic triangular wing.— In the case of the subsonic triangular wing, equation (37) becomes

$$C_L = \frac{1}{m c_o^2} \int_0^{c_o} dx \int_{-mx}^{mx} \frac{4 \alpha m^2 x}{\sqrt{m^2 x^2 - y^2}} f_1 \left(\frac{x}{c_o} \right) dy$$

and this becomes (since $A = 4m$)



$$\frac{C_L}{\alpha A} = \pi \int_0^1 x_0 f_1(x_0) dx_0 \quad (39)$$

The numerical evaluation of equation (39) is not difficult since $x_0 f_1(x_0)$ has the variation shown in the sketch.

Supersonic rectangular wing.— For values of $c_0 < 2s\beta$ the exact value of the lift coefficient on a rectangular wing flying at supersonic speeds has been obtained and can be written in the form:

For $A_r > 1$

$$\frac{C_L}{\alpha A} = \frac{4A_r - 2}{A_r^2} \quad (40)$$

When $A_r < 1$ equation (37) must be used in connection with equation (24) and there results

$$C_L = \frac{1}{2s c_0} \int_0^{c_0} d\tilde{x} \int_{-s}^s \frac{4\alpha}{s\beta} f_4\left(\frac{x}{s\beta}\right) \sqrt{s^2 - y^2} dy$$

which reduces to

$$C_L = \frac{\alpha\pi}{c_0\beta} \int_0^{c_0} f_4\left(\frac{x}{s\beta}\right) dx$$

and this can be written in the form

$$\frac{C_L}{\alpha A} = \frac{\pi}{A_r c_0} \int_0^{c_0} f_4\left(\frac{2x}{c_0 A_r}\right) dx$$

which becomes, if $x_2 = \frac{2x}{c_0 A_r}$,

for $A_r < 1$

$$\frac{C_L}{\alpha A} = \frac{\pi}{2} \int_0^{\frac{2}{A_r}} f_4(x_2) dx_2 \quad (41)$$

Subsonic rectangular wing.— The equation for the loading on a subsonic rectangular wing, equation (14), placed in the formula for lift coefficient yields

$$C_L = \frac{1}{2sc_0} \int_0^{c_0} dx \int_{-s}^s \frac{4\alpha}{c_0} f_2\left(\frac{x}{c_0}\right) \sqrt{s^2 - y^2} dy$$

which becomes

$$\frac{C_L}{\alpha A} = \frac{\pi}{2} \int_0^1 f_2(x_0) dx_0 \quad (42)$$

The evaluation of equation (42) by numerical means requires special consideration since $f_2(x_0)$ approaches infinity at the leading edge as shown in figure 4. To this end, rewrite equation (42) in the form

$$\frac{C_L}{\alpha A} = \frac{\pi}{2} \int_0^\epsilon f_2(x_0) dx_0 + \frac{\pi}{2} \int_\epsilon^1 f_2(x_0) dx_0 \quad (43)$$

and equation (B4) in the appendix (for the special case in which $x_0=1$) in the form

$$1 = \frac{1}{2\pi} \int_0^\epsilon f_2(x_0) \left[\pi + \frac{A_r E}{k(1-x_0)} \right] dx_0 + \frac{1}{2\pi} \int_\epsilon^1 f_2(x_0) \left[\pi + \frac{A_r E}{k(1-x_0)} \right] dx_0 \quad (44)$$

An application of the mean-value theorem yields

$$\int_0^\epsilon f_2(x_0) dx_0 = \frac{1}{\left[\pi + \frac{A_r E \theta}{k_\theta(1-\theta)} \right]} \left\{ 2\pi - \int_\epsilon^1 f_2(x_0) \left[\pi + \frac{A_r E}{k(1-x_0)} \right] dx_0 \right\} \quad (45)$$

where $E\theta$ has the modulus k_θ which equals $A_r / \sqrt{4(1-\theta^2) + A_r^2}$ and where $0 < \theta < \epsilon$. The combination of equations (43) and (45) yields an expression for the lift coefficient involving only the load distribution from a distance ϵ/c_0 back of the leading edge to the trailing edge.

Pitching Moment

By definition the pitching-moment coefficient about the apex or leading edge and based on the root chord can be written

$$C_m = -\frac{1}{Sc_0} \iint_S x \frac{\Delta p}{q} dx dy \quad (46)$$

Equation (46) will be applied to the various loadings which have been studied.

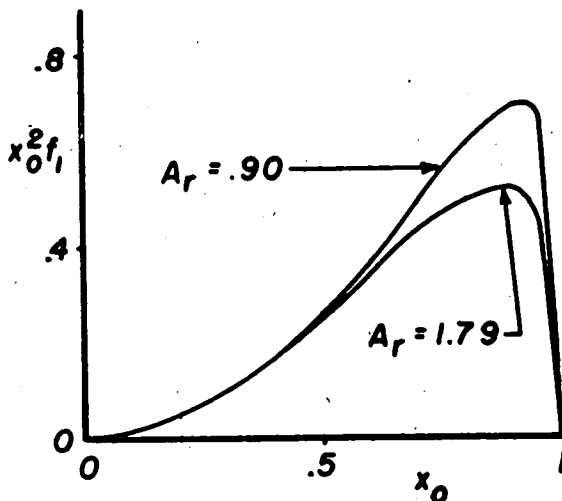
Supersonic triangular wing.— The exact linearized value for the pitching-moment coefficient on a triangular wing flying at supersonic speeds has been derived elsewhere and can be written in the form

$$\frac{C_m}{\alpha A} = -\frac{\pi}{3E} \quad (47)$$

Subsonic triangular wing.— The derivation of the pitching moment on a subsonic triangular wing proceeds in the same manner as the derivation of lift and there results

$$\frac{C_m}{\alpha A} = -\pi \int_0^1 x_0^2 f_1(x_0) dx_0 \quad (48)$$

This expression can be easily integrated numerically since $x_0^2 f_1(x_0)$ varies as the sketch indicates.



Supersonic rectangular wing.— For values of reduced aspect ratio A_r greater than 1 the pitching-moment coefficient on a rectangular wing is given by the equation,

for $A_r > 1$

$$\frac{C_m}{\alpha A} = -\frac{6A_r - 4}{3A_r^2} \quad (49)$$

When $A_r < 1$ the solution to the integral equation must be used and the final expression can be written

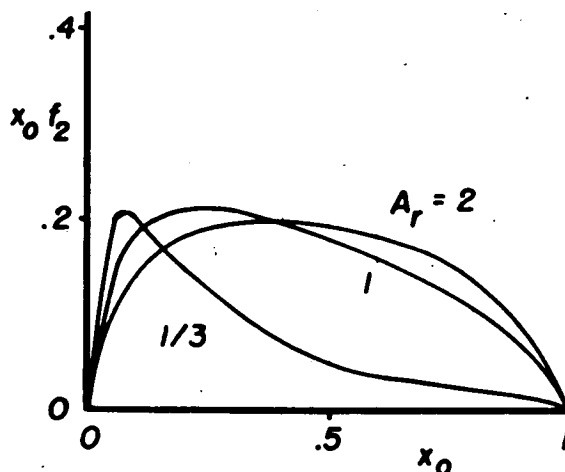
$$\frac{C_m}{\alpha A} = -\frac{\pi A_r}{4} \int_0^{2/A_r} x_2^2 f_4(x_2) dx_2 \quad (50)$$

Subsonic rectangular wing.— The equation for the pitching-moment coefficient on a subsonic rectangular wing follows in the same manner as did that for the lift coefficient.

Hence,

$$\frac{C_m}{\alpha A} = -\frac{\pi}{2} \int_0^1 x_0 f_2(x_0) dx_0 \quad (51)$$

and, since the variation of $x_0 f_2(x_0)$ is as indicated in the sketch, the numerical integration of equation (51) is simple.



Center of Pressure

Since the pitching moment is based on the root chord, the center of pressure of all wing plan forms can be written

$$\frac{x_{c.p.}}{c_o} = \frac{C_m}{C_L} \quad (52)$$

Discussion of Results

Figures 5 and 6 show the variation of the lift coefficient and center of pressure for triangular and rectangular wings for the range in which the reduced aspect ratio A_r is small. For the triangular wing the differences between the subsonic and supersonic cases are not large in the interval of A_r shown; the subsonic wing develops somewhat less lift and the center of pressure moves forward as A_r increases. The characteristics of the rectangular wing, however, show a large variation in passing through the speed of sound.

The subsonic rectangular wing has a variation of C_L/α with A_r which is almost identical with that for the subsonic triangular wing. Unlike the triangular wing, however, the curve for $x_{c.p.}/c_o$ on the rectangular wing shows that this lift is carried farther and farther forward from the quarter-chord position at $M_0 = 0$ all the way to the leading edge at $M_0 = 1$.

As the speed is further increased and the rectangular wing enters the supersonic speed range, the magnitude of the lift oscillates about the curve for the subsonic case until a reduced aspect ratio of about 0.5 is reached and then rises to a maximum at about the point where A_r equals 1. The exact curve (obtained by linearized lifting-surface theory) for values of A_r greater than one is shown as a dotted line for the purpose of comparison.

The variation of the center of pressure on a supersonic rectangular wing indicates that the wing is unstable for all positions of the pivot point behind the leading edge for values of A_r around 0.4, the center of pressure, in such a range, having moved forward of the wing leading edge. As A_r increases past the value 0.5, however, the center of pressure moves back along the wing and rapidly approaches the midchord point, its location according to two-dimensional linearized theory.

CONCLUDING REMARKS

A theoretical investigation has been made of the correction to slender-wing theory which accounts for the effects of compressibility and the chordwise gradients in velocity. Integral equations were developed and numerically evaluated for triangular and rectangular plan forms in both subsonic and supersonic flow.

In the case of the triangular plan form, the value of the lift coefficient predicted by slender-wing theory was reduced by an amount which increased with increasing aspect ratio as was to be expected. At a reduced aspect ratio of 1.0, this correction amounted to 6 percent for both subsonic and supersonic flow, but, at a reduced aspect ratio of 2.0, the correction had increased to 21 percent in the case of subsonic flow and 17 percent in the case of supersonic flow.

The center of pressure of a triangular wing in supersonic flow remained constant as predicted by slender-wing theory; in subsonic flow, however, there was a slight forward shifting of the center of pressure with increasing aspect ratio which amounted to 6 percent of a root chord length at a reduced aspect ratio of 2.0.

In the case of the rectangular plan form in subsonic flow, the correction to the lift coefficient due to a consideration of the chordwise and compressibility effects was the same as for the triangular plan form. In supersonic flow, below a reduced aspect ratio of 0.5, the value of the lift coefficient oscillated about the constant value predicted by slender-wing theory. Above this value the lift coefficient was increased, reaching a maximum correction of 32 percent at a reduced aspect ratio of 1.0. At $A_r = 2.0$ the lift coefficient was again decreased by 9 percent.

According to slender-wing theory, the center of pressure of a rectangular plan form is located on the leading edge. In the subsonic case, the corrections shifted the position of the center of pressure back from the leading edge as the aspect ratio was increased. This shift amounted to 19 percent of a chord length at a reduced aspect ratio of 2.0. In the supersonic case, a consideration of the chordwise and compressibility effects indicated that the wing was unstable for a pivot point located at

the leading edge around a reduced aspect ratio of 0.4. As the aspect ratio increased, the center of pressure moved back of the leading edge toward the midchord position.

Ames Aeronautical Laboratory,
National Advisory Committee for Aeronautics,
Moffett Field, Calif., Nov. 28, 1950.

APPENDIX A

EVALUATION OF SPECIAL INTEGRALS

THE INTEGRAL I_1

The evaluation of I_1 will be discussed first for the case in which $x > x_1$ and second for the case in which $x < x_1$.

Case 1, $x > x_1$

It is possible to write I_1 in the form

$$I_1 = m \int_{\mu_0}^{\mu_1} \frac{\sqrt{\mu_0^2 + \beta^2 m^2 \eta^2}}{\eta \sqrt{(\eta - \mu_0)(\mu_1 - \eta)}} d\eta \quad (A1)$$

where $\mu_0 = m(x - x_1)$ and $\mu_1 = m(x + x_1)$. The linear term in the lower radical of the integrand can be eliminated by the transformation $\eta = (\sigma + \delta t)/(1 + t)$, and the integral becomes

$$I_1 = \frac{m(\delta - \sigma)}{\sqrt{(\mu_0 - \sigma)(\sigma - \mu_1)}} \int_{\frac{\sigma - \mu_1}{\mu_1 - \delta}}^{\frac{\sigma - \mu_0}{\mu_0 - \delta}} \frac{\sqrt{(\mu_0^2 + \sigma^2 \beta^2 m^2) + (\mu_0^2 + \delta^2 \beta^2 m^2) t^2}}{(1+t)(\sigma + \delta t) \sqrt{1 - \left(\frac{\mu_1 - \delta}{\sigma - \mu_1}\right) \left(\frac{\delta - \mu_0}{\sigma - \mu_0}\right) t^2}} dt \quad (A2)$$

where

$$\sigma = \frac{-\mu_0(\mu_0 - \beta^2 m^2 \mu_1) + \mu_0 \sqrt{(1 + \beta^2 m^2)(\mu_0^2 + \beta^2 m^2 \mu_1^2)}}{\beta^2 m^2 (\mu_1 + \mu_0)} \quad (A3)$$

and

$$\delta = \frac{-\mu_0(\mu_0 - \beta^2 m^2 \mu_1) - \mu_0 \sqrt{(1 + \beta^2 m^2)(\mu_0^2 + \beta^2 m^2 \mu_1^2)}}{\beta^2 m^2 (\mu_1 + \mu_0)} \quad (A4)$$

The expression for σ and δ may be combined to give the useful identities

$$\mu_0^2 = -\sigma \delta \beta^2 m^2$$

$$(\mu_0 - \sigma)(\delta - \mu_1) + (\mu_1 - \sigma)(\delta - \mu_0) = 0$$

Using fundamental properties of even and odd functions, equation (A2) may be reduced to the form

$$I_1 = 2m \sqrt{\frac{\mu_0^2 + \sigma^2 \beta^2 m^2}{(\mu_1 - \delta)(\mu_0 - \delta)}} \int_0^1 \left[\left(\frac{1}{1 + \frac{\sigma k^2}{\delta k'^2} \omega^2} - \frac{\delta/\sigma}{1 + \frac{\delta k^2}{\sigma k'^2} \omega^2} \right) \frac{1}{k'} \right. \\ \left. \sqrt{\frac{k'^2 + k^2 \omega^2}{1 - \omega^2}} \right] d\omega$$

by the substitution

$$\omega = \left| \frac{\mu_1 - \delta}{\mu_1 - \sigma} \right| t$$

and where

$$k^2 = \frac{(\mu_1 - \sigma)^2 \delta}{(\mu_1^2 - \sigma \delta)(\delta - \sigma)}$$

$$\frac{k^2}{k'^2} = -\frac{\delta}{\sigma} \left(\frac{\mu_1 - \sigma}{\mu_1 - \delta} \right)^2$$

By introducing the Jacobian elliptic functions in the transformations $\omega = \text{cnu}$, the integral reduces to

$$I_1 = \frac{2m}{k} \sqrt{\frac{\mu_0^2 + \delta^2 \beta^2 m^2}{(\mu_1 - \sigma)(\sigma - \mu_0)}} \int_0^K \left(\frac{v_1^2}{1 + v_1^2 \text{sn}^2 u} - \frac{\frac{\sigma}{\delta} v_2^2}{1 + v_2^2 \text{sn}^2 u} \right) \text{dn}^2 u \, du \quad (\text{A5})$$

where

$$v_1^2 = \frac{-\left(\frac{\sigma}{\delta}\right) k^2}{k'^2 + \frac{\sigma}{\delta} k^2} > 0 \quad (\text{A6})$$

and

$$v_2^2 = \frac{-\left(\frac{\delta}{\sigma}\right) k^2}{k'^2 + \frac{\delta}{\sigma} k^2} > 0 \quad (A7)$$

The integration may now be completed and

$$\begin{aligned} I_1 &= \frac{2m}{k} \sqrt{\frac{\mu_0^2 + \delta^2 \beta^2 m^2}{(\mu_1 - \sigma)(\sigma - \mu_0)}} \left[v_1 \sqrt{\frac{v_1^2 + k^2}{1 + v_1^2}} G\left(\frac{v_1}{\sqrt{v_1^2 + k^2}}\right) - \right. \\ &\quad \left. \frac{\sigma}{\delta} v_2 \sqrt{\frac{v_2^2 + k^2}{1 + v_2^2}} G\left(\frac{v_2}{\sqrt{v_2^2 + k^2}}\right) \right] \\ &= 2m \left[\beta m G\left(\frac{v_1}{\sqrt{v_1^2 + k^2}}\right) + \sqrt{\frac{\mu_0}{\mu_1}} G\left(\frac{v_2}{\sqrt{v_2^2 + k^2}}\right) \right] \quad (A8) \end{aligned}$$

where

$$G(x) = EF'(x) + KE'(x) - KF'(x) \quad (A9)$$

the modulus of the elliptic integrals being k or k' .

Case 2, $x < x_1$

The procedure for obtaining the solution for I_1 in this case is identical to that followed in case 1 except that in order to fulfill the condition that $t > -1$, σ and δ must be defined in the following manner:

$$\delta = \frac{-\mu_0(\mu_0 - \beta^2 m^2 \mu_1) + \mu_0 \sqrt{(1 + \beta^2 m^2)(\mu_0^2 + \beta^2 m^2 \mu_1^2)}}{\beta^2 m^2(\mu_1 + \mu_0)} \quad (A10)$$

$$\sigma = \frac{-\mu_0(\mu_0 - \beta^2 m^2 \mu_1) - \mu_0 \sqrt{(1 + \beta^2 m^2)(\mu_0^2 + \beta^2 m^2 \mu_1^2)}}{\beta^2 m^2 (\mu_1 + \mu_0)} \quad (A11)$$

In this case it can be shown that in equation (A5) $v_1 > 0$ and $v_2 < -1$, and the solution for I_1 is

$$I_1 = 2m \left\{ \beta m G \left(\frac{v_1}{\sqrt{v_1^2 + k^2}} \right) + \beta m \sqrt{\frac{\delta \sigma}{\mu_0 \mu_1}} \left[\text{KE} \left(\frac{-1}{v_2} \right) - \text{EF} \left(\frac{-1}{v_2} \right) \right] + \right. \\ \left. \frac{\sigma}{\delta} k \sqrt{\frac{\mu_0^2 + \delta^2 \beta^2 m^2}{(\mu_1 - \sigma)(\sigma - \mu_0)}} K \right\} \quad (A12)$$

where $G(x)$ is defined as in equation (A9).

THE INTEGRAL I_2

Writing I_2 in the form

$$I_2 = 2 \int_0^s \sqrt{\frac{(x-x_1)^2 + y_1^2 \beta^2}{s^2 - y_1^2}} dy_1 \quad (A13)$$

and setting

$$\frac{y_1}{s} = \text{cnu}, \quad k = \frac{\beta s}{\sqrt{(x-x_1)^2 + \beta^2 s^2}}$$

I_2 can be integrated to give

$$I_2 = 2\beta s \int_0^K \frac{dn^2 u du}{k} = \frac{2\beta s E}{k} \quad (A14)$$

THE INTEGRAL I_3

Case 1, $\theta_0 \mu_1 < \mu_0 < \mu_1$

Writing I_3 in the form

$$I_3 = \theta_0 \int_{\mu_0}^{\mu_1} \frac{d\eta}{\eta} \sqrt{\frac{\frac{\mu_0^2}{\theta_0^2} - \eta^2}{(\mu_1 - \eta)(\eta - \mu_0)}} \quad (A15)$$

and making the transformation

$$\text{sn}^2 u = \frac{2}{(1 - \theta_0^2)k^2} \frac{\eta - \mu_0}{\eta + \frac{\mu_0}{\theta_0}} \quad (A16)$$

where

$$k^2 = \frac{2\theta_0}{1 - \theta_0} \frac{\mu_1 - \mu_0}{\mu_1\theta_0 + \mu_0} \quad (A17)$$

reduces equation (A15) to the form

$$I_3 = (1 + \theta_0)k \sqrt{\frac{2\mu_0}{\theta_0(\mu_1 - \mu_0)}} \left(\int_0^K \frac{du}{1 + \frac{1 - \theta_0}{2\theta_0} k^2 \text{sn}^2 u} - \int_0^K \frac{\theta_0 du}{1 - \frac{1 - \theta_0}{2} k^2 \text{sn}^2 u} \right)$$

The integration may now be completed and

$$I_3 = \sqrt{\frac{2\mu_0\theta_0}{\mu_1 - \mu_0}} k \left\{ (1 - \theta_0)K + \frac{\sqrt{1 - \theta_0^2} G\left(\sqrt{\frac{1 - \theta_0}{1 + \theta_0}}\right)}{\theta_0 \sqrt{1 + \frac{1 - \theta_0}{2\theta_0} k^2}} - \frac{\sqrt{1 - \theta_0^2}}{\sqrt{1 - \frac{1 - \theta_0}{2} k^2}} \left[\text{KE}\left(\sqrt{\frac{1 - \theta_0}{2}}\right) - \text{EF}\left(\sqrt{\frac{1 - \theta_0}{2}}\right) \right] \right\} \quad (A18)$$

Case 2, $0 < \mu_0 < \theta_0 \mu_1$

In this case

$$I_3 = \theta_0 \int_{\mu_0}^{\frac{\mu_0}{\theta_0}} \sqrt{\frac{\frac{\mu_0^2}{\theta_0^2} - \eta^2}{(\mu_1 - \eta)(\eta - \mu_0)}} \frac{d\eta}{\eta} \quad (A19)$$

and the transformation

$$\operatorname{sn}^2 u = \frac{2}{1-\theta_0} \frac{\eta - \mu_0}{\eta + \frac{\mu_0}{\theta_0}}$$

is made where

$$k^2 = \frac{1-\theta_0}{2} \frac{\mu_1 + \frac{\mu_0}{\theta_0}}{\mu_1 - \mu_0}$$

Equation (A19) then becomes

$$I_3 = (1+\theta_0) \sqrt{\frac{2\mu_0}{\theta_0(\mu_1-\mu_0)}} \left(\int_0^K \frac{du}{1 + \frac{1-\theta_0}{2\theta_0} \operatorname{sn}^2 u} - \int_0^K \frac{\theta_0 du}{1 - \frac{1-\theta_0}{2} \operatorname{sn}^2 u} \right)$$

The integration can be completed so that

$$I_3 = (1+\theta_0) \sqrt{\frac{2\mu_0}{\theta_0(\mu_1-\mu_0)}} \left\{ \theta_0 K \left(\frac{2k^2}{1-\theta_0+2\theta_0 k^2} - 1 \right) + \sqrt{\frac{2\theta_0(1-\theta_0^2)}{1-\theta_0+2\theta_0 k^2}} \frac{G\left(\sqrt{\frac{1-\theta_0}{1-\theta_0+2\theta_0 k^2}}\right)}{1+\theta_0} - \frac{\theta_0}{1+\theta_0} \sqrt{\frac{2(1-\theta_0^2)}{2k^2-1+\theta_0}} \left[\operatorname{KE}\left(\frac{1}{k} \sqrt{\frac{1-\theta_0}{2}}\right) - \operatorname{EF}\left(\frac{1}{k} \sqrt{\frac{1-\theta_0}{2}}\right) \right] \right\} \quad (\text{A20})$$

THE INTEGRAL I_4

Case 1, $0 \leq x_1 \leq x - \beta s$

The integral I_4 can be written

$$I_4 = 2 \int_0^s \sqrt{\frac{(x-x_1)^2 - \beta^2 y_1^2}{s^2 - y_1^2}} dy_1 \quad (\text{A21})$$

When the transformation $\text{snu} = y_1/s$ is made, the expression may be integrated to give

$$I_4 = 2(x-x_1) \int_0^K \text{dn}^2 u \, du = 2(x-x_1)E_1 \quad (\text{A22})$$

where

$$k_1^2 = \frac{s^2 \beta^2}{(x-x_1)^2} \quad (\text{A23})$$

Case 2, $x-\beta s \leq x_1 \leq x$

In this case I_4 can be written

$$I_4 = 2 \int_0^{\frac{x-x_1}{\beta}} \sqrt{\frac{(x-x_1)^2 - \beta^2 y_1^2}{s^2 - y_1^2}} \, dy_1 \quad (\text{A24})$$

The transformation $\text{snu} = \beta y_1/(x-x_1)$ applied to equation (A24) yields

$$I_4 = 2 \int_0^K \frac{(x-x_1)^2}{\beta s} \text{cn}^2 u \, du = 2k_2(x-x_1)B_2 \quad (\text{A25})$$

where

$$k_2 = \frac{x-x_1}{\beta s} \quad (\text{A26})$$

and

$$B_2 = \frac{E_2 - k_2'^2 K_2}{k_2^2} \quad (\text{A27})$$

APPENDIX B

NUMERICAL SOLUTION OF INTEGRAL EQUATIONS

SUBSONIC TRIANGULAR WING

Since the integral I_1 is a function only of the ratio x_1/x , equation (10) can be written for $\bar{w} = w_0$

$$1 = \frac{1}{2} \int_0^1 \xi f_1 \left(\frac{x_\xi}{c_0} \right) \frac{d\xi}{\sqrt{1-\xi^2}} + \frac{1}{2\pi} \int_0^{\frac{c_0}{x}} \frac{\xi}{1-\xi} I_1(\xi) f_1 \left(\frac{x_\xi}{c_0} \right) d\xi \quad (B1)$$

where $\xi = x_1/x$. It is now assumed that $f(x_\xi/c_0)$ may be considered constant over small intervals. This reduces the solution of the integral equation to the elementary problem of solving a system of simultaneous algebraic equations. On the basis of such an assumption equation (B1) becomes

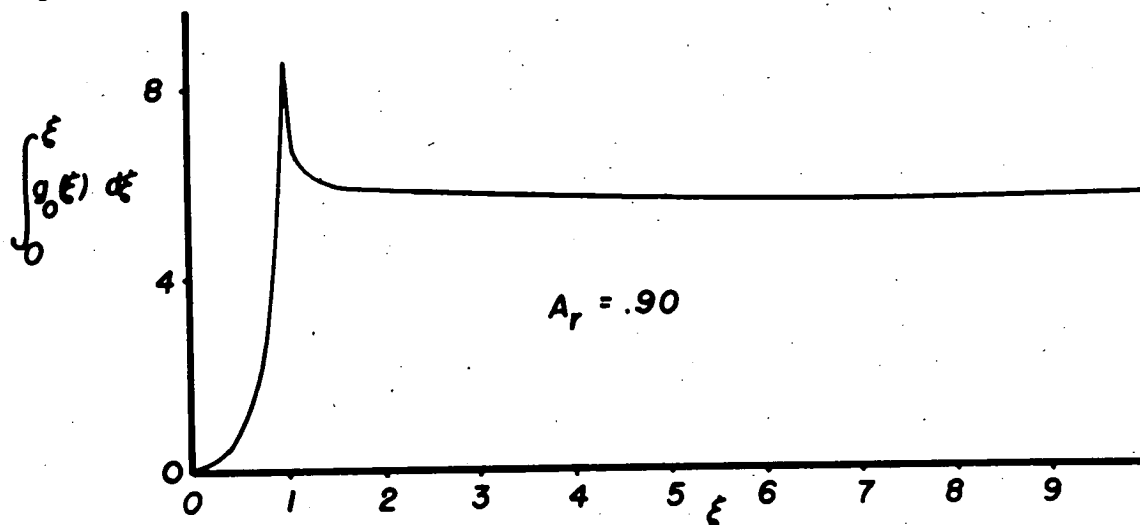
$$1 = \frac{1}{2\pi} \left\{ \sum_{i=1}^n f_1 \left(\frac{2i-1}{2n} \right) \left[\int_{\frac{2(i-1)}{2j-1}}^{\frac{2i}{2j-1}} g_0(\xi) d\xi \right] \right\} \quad j=1,2,3 \dots n \quad (B2)$$

where

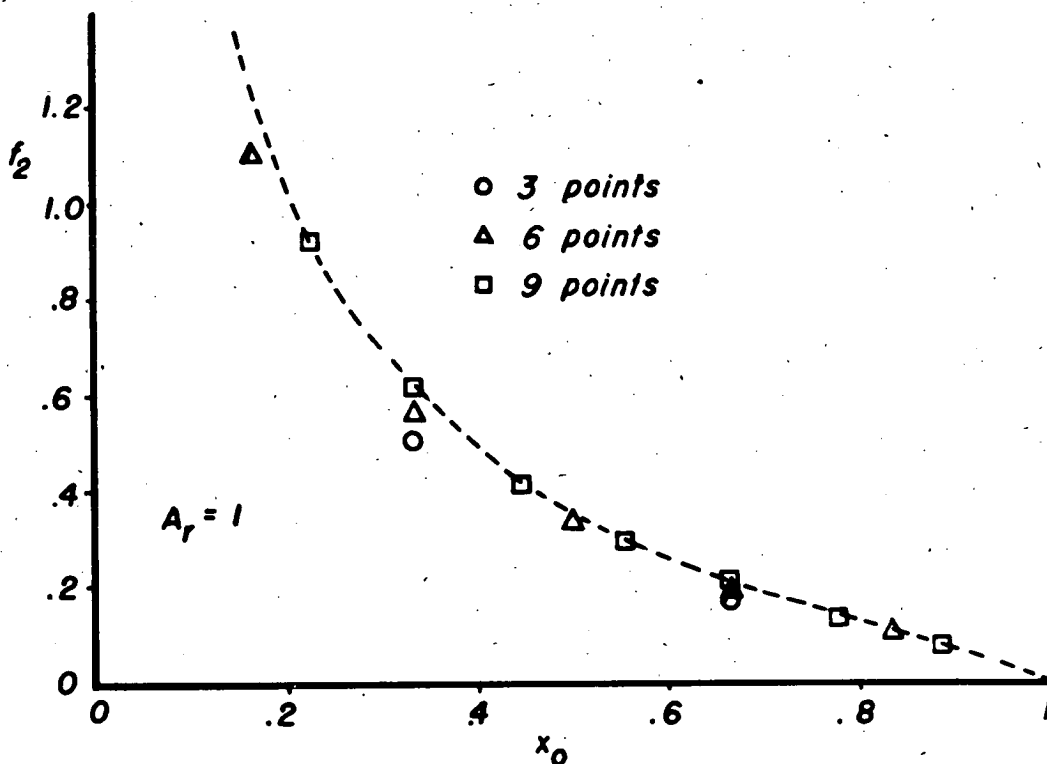
$$\left. \begin{aligned} g_0(\xi) &= \frac{\pi \xi}{\sqrt{1-\xi^2}} + \frac{\xi}{1-\xi} I_1(\xi) & 0 < \xi < 1 \\ g_0(\xi) &= \frac{\xi}{1-\xi} I_1(\xi) & 1 < \xi < \frac{c_0}{x} \end{aligned} \right\} \quad (B3)$$

The function $g_0(\xi)$ can be integrated by numerical means, and it is convenient to make a plot such as is shown in the sketch in which each

ordinate represents the value of $g_0(\xi)$ integrated over the interval 0 to ξ .



Systems of simultaneous equations were obtained for values of n equal to 3, 6, and 9. Solutions were found using the Gauss-Seidel method (for which the simultaneous equations were well suited) and the convergence was rapid as the sketch indicates.



SUBSONIC RECTANGULAR WING

Substituting the value of I_2 given by equation (A14) into equation (16), one has for $w = w_0$

$$1 = \frac{1}{2\pi} \int_0^1 g\left(\frac{x-x_1}{c_0}\right) f_2\left(\frac{x_1}{c_0}\right) d\left(\frac{x_1}{c_0}\right) \quad (B4)$$

where

$$g\left(\frac{x-x_1}{c_0}\right) = \pi + \frac{A_r E}{\left(\frac{x-x_1}{c_0}\right)^k}$$

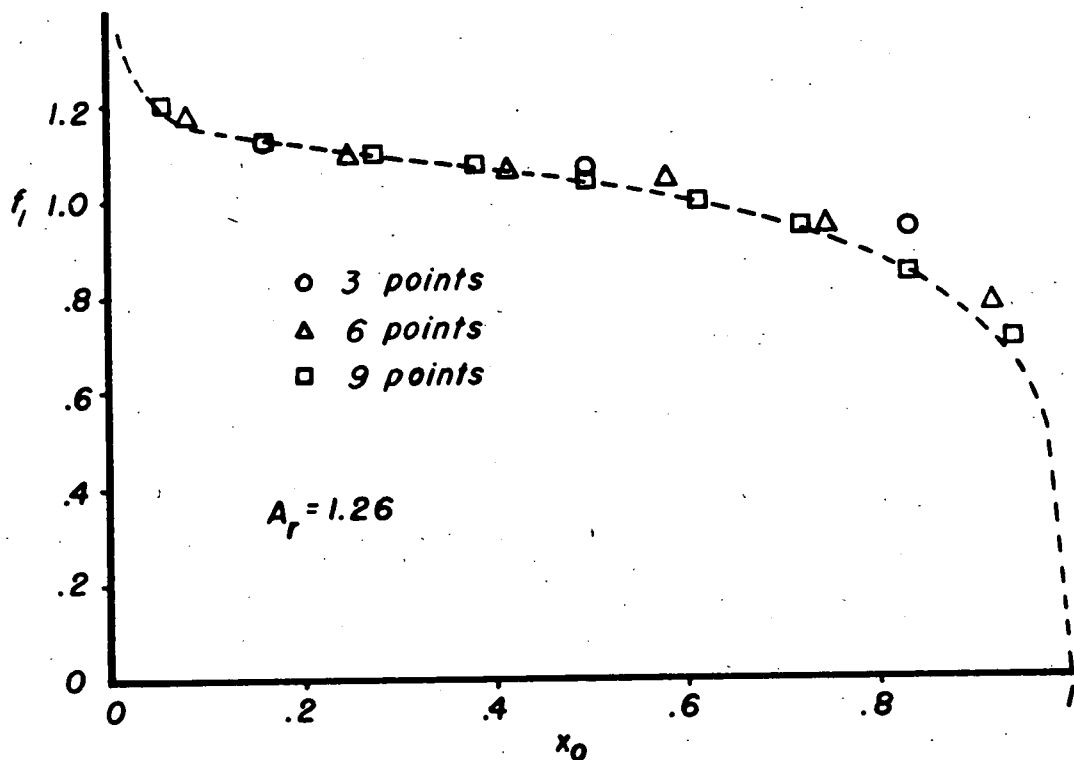
and where

$$k = \frac{\beta s}{\sqrt{(x-x_1)^2 + \beta^2 s^2}} = \frac{A_r}{\sqrt{4\left(\frac{x-x_1}{c_0}\right)^2 + A_r^2}}$$

A satisfactory numerical solution of equation (B4) requires the solution of the system of simultaneous equations of the form

$$1 = \frac{1}{2\pi} \sum_{i=1}^n \frac{1}{2n} \left\{ f_2(0) g\left(\frac{2i-1}{2n} - 0\right) + 2 \left[f_2\left(\frac{1}{n}\right) g\left(\frac{2i-1}{2n} - \frac{1}{n}\right) + \right. \right. \\ \left. \left. f_2\left(\frac{2}{n}\right) g\left(\frac{2i-1}{2n} - \frac{2}{n}\right) + \dots + f_2\left(\frac{n-1}{n}\right) g\left(\frac{2i-1}{2n} - \frac{n-1}{n}\right) \right] + \right. \\ \left. f_2(1) g\left(\frac{2i-1}{2n} - 1\right) \right\} \quad (B5)$$

The convergence of the solutions to equation (B5) is indicated in the sketch where the value of n was successively taken to be 3, 6, and 9.



SUPERSONIC RECTANGULAR WING

Equation (25) can be written when $w = w_0$ as

$$1 = f_4\left(\frac{x}{s\beta}\right) + \int_0^x g_1\left(\frac{x-x_1}{s\beta}\right) f_4\left(\frac{x_1}{s\beta}\right) \frac{dx_1}{s\beta} \quad (B6)$$

where from equations (A22) and (A25)

$$g_1\left(\frac{x-x_1}{s\beta}\right) = \begin{cases} \frac{2}{\pi} E_1 & \frac{x-x_1}{\beta s} \geq 1 \\ \frac{2}{\pi} k_2 B_2 & \frac{x-x_1}{\beta s} \leq 1 \end{cases} \quad (B7)$$

and where

$$k_1 = \frac{s\beta}{x-x_1} \quad k_2 = \frac{x-x_1}{s\beta}$$

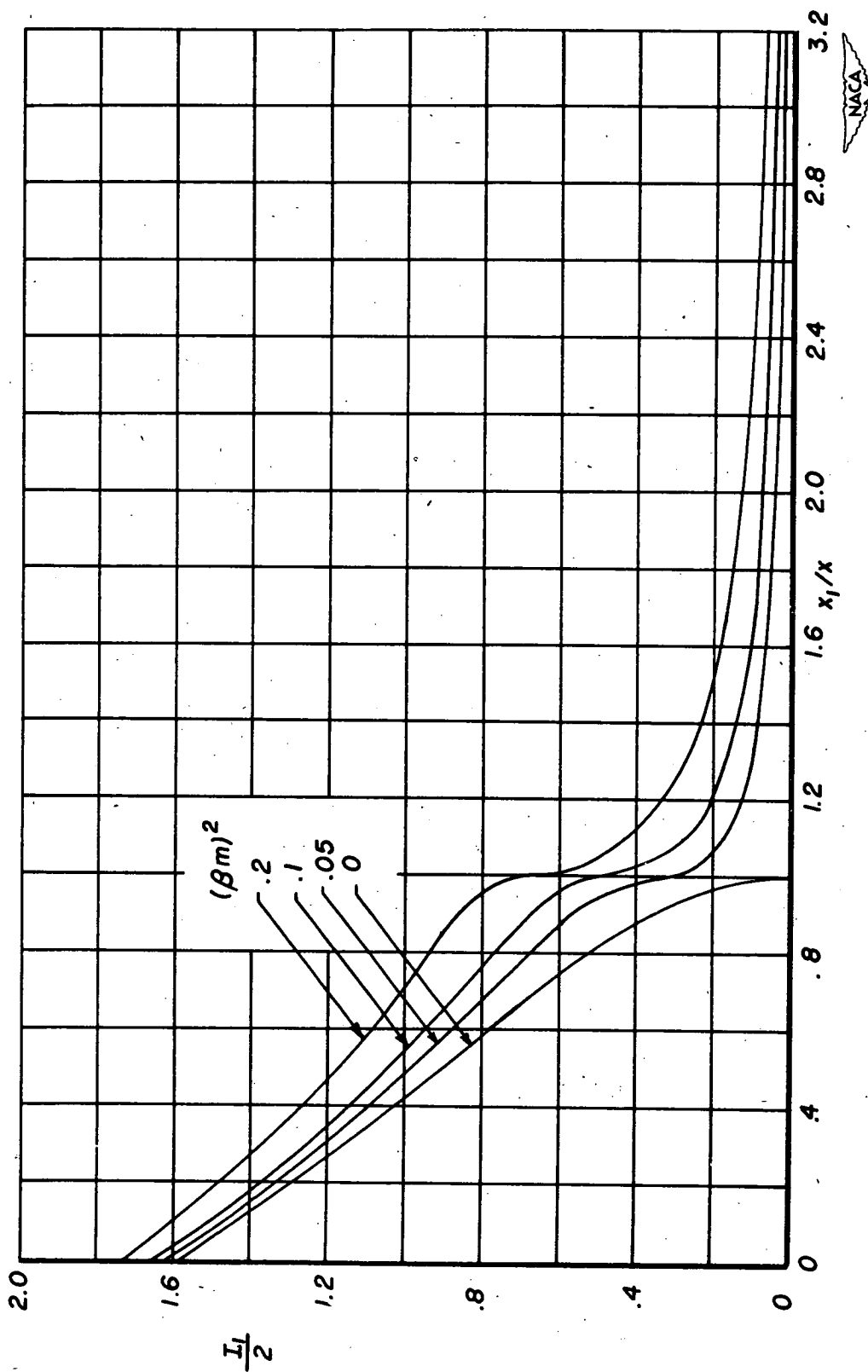
By the application of the trapezoidal rule for numerical integration to equation (B6), it is possible to write $f_4(x/s\beta)$ explicitly as

$$f_4 \left(\frac{x}{\beta s} \right) = 1 - \frac{1}{2} \Delta \left(\frac{x}{\beta s} \right) \left[g_1(0) + 2 \sum_{i=1}^n g_1 \left(\frac{x}{\beta s} \right)_i f \left(\frac{x}{\beta s} \right)_i \right] \quad (B8)$$

where $\Delta(x/\beta s)$ is the interval of the trapezoid.

REFERENCES

1. Jones, Robert T.: Properties of Low-Aspect-Ratio Pointed Wings at Speeds Below and Above the Speed of Sound. NACA Rep. 835, 1946.
2. Ribner, Herbert S.: The Stability Derivatives of Low-Aspect-Ratio Triangular Wings at Subsonic and Supersonic Speeds. NACA TN 1423, 1947.
3. Spreiter, John R.: Aerodynamic Properties of Slender Wing-Body Combinations at Subsonic, Transonic, and Supersonic Speeds. NACA TN 1662, 1948.
4. Heaslet, Max A., Lomax, Harvard, and Spreiter, John R.: Linearized Compressible-Flow Theory for Sonic Flight Speeds. NACA TN 1824, 1949.
5. Lomax, Harvard, and Heaslet, Max. A.: Linearized Lifting-Surface Theory for Swept-Back Wings With Slender Plan Forms. NACA TN 1992, 1949.
6. Lamb, Sir Horace: Hydrodynamics. Dover Publications (New York), 6th ed., p. 60, 1945.
7. Lomax, Harvard, Heaslet, Max. A., and Fuller, Franklyn B.: Formulas for Source, Doublet, and Vortex Distributions in Supersonic Wing Theory. NACA TN 2252, 1950.
8. Prandtl, L.: Recent Work on Airfoil Theory. NACA TM 962, 1940.
9. Heaslet, Max. A., Lomax, Harvard, and Jones, Arthur L.: Volterra's Solution of the Wave Equation as Applied to Three-Dimensional Supersonic Airfoil Problems. NACA TR 889, 1947.
10. Stewart, H. J.: The Lift of a Delta Wing at Supersonic Speeds. Quarterly of Applied Mathematics, vol. IV, no. 3, Oct. 1946, pp. 246-254.
11. Brown, Clinton E.: Theoretical Lift and Drag of Thin Triangular Wings at Supersonic Speeds. NACA Rep. 839, 1946.
12. Gurdvich, M. I.: Lift Force of an Arrow-Shaped Wing. NACA TM 1245, Oct. 1949.

Figure 1.- Variation of I_1 with x_1/x .

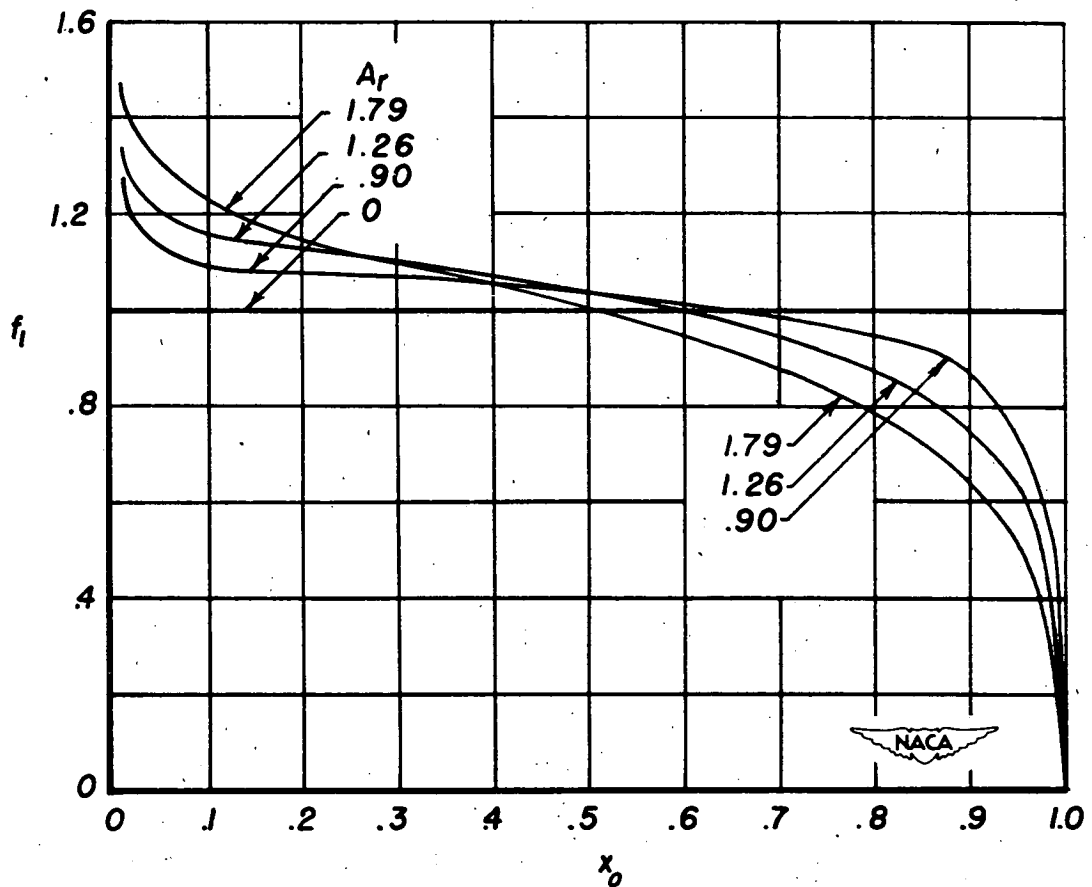


Figure 2.- Variation of chordwise correction factor f_l for subsonic triangular wing. $C_{L\alpha} = \pi A \int_0^1 x_0 f_l(x_0) dx_0$.

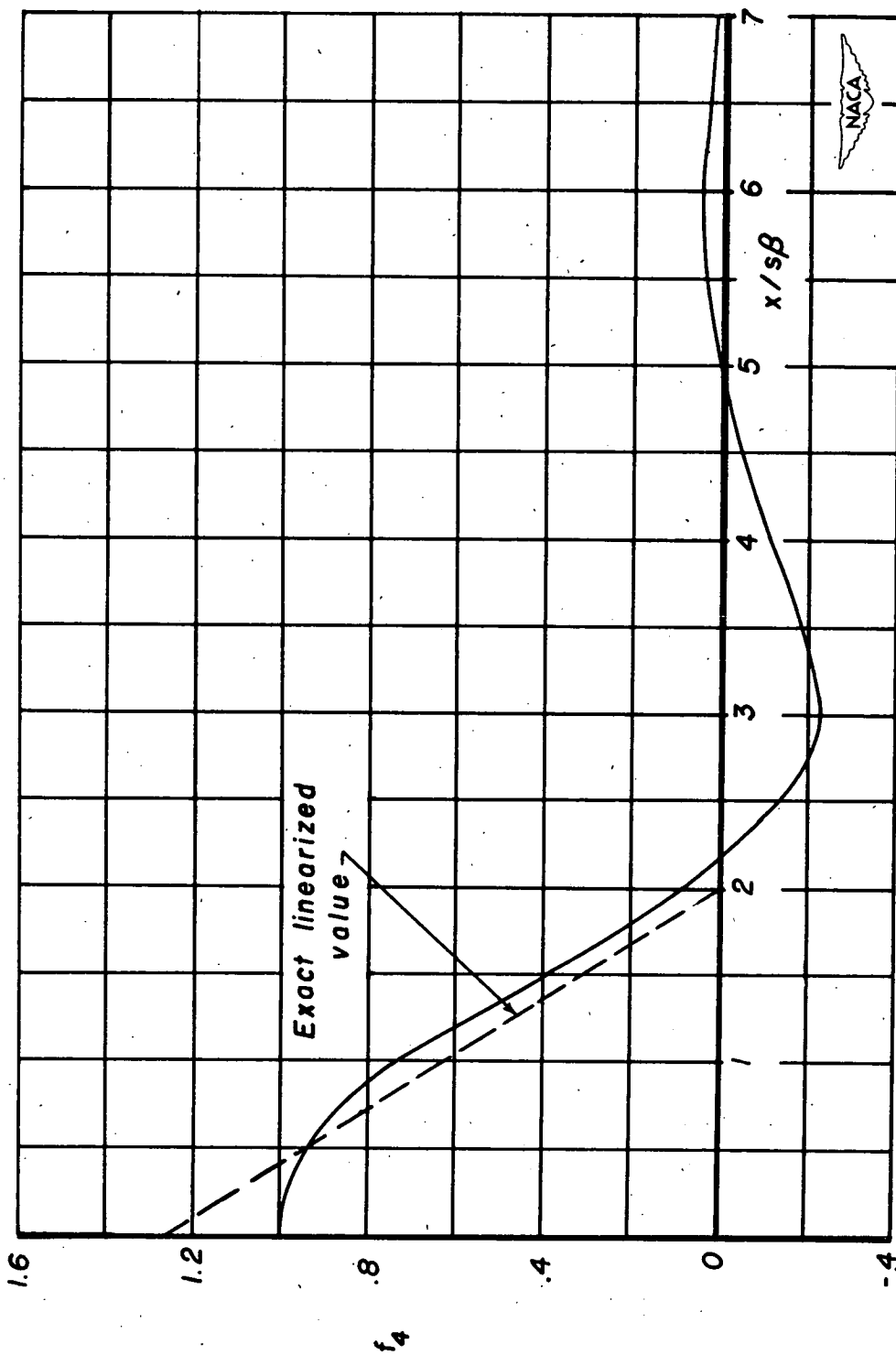


Figure 3.— Variation of chordwise correction factor f_4 for supersonic rectangular wing. $C_{L\alpha} = \frac{\pi A}{2} \int_0^{3/4} f_4(x_2) dx_2$.

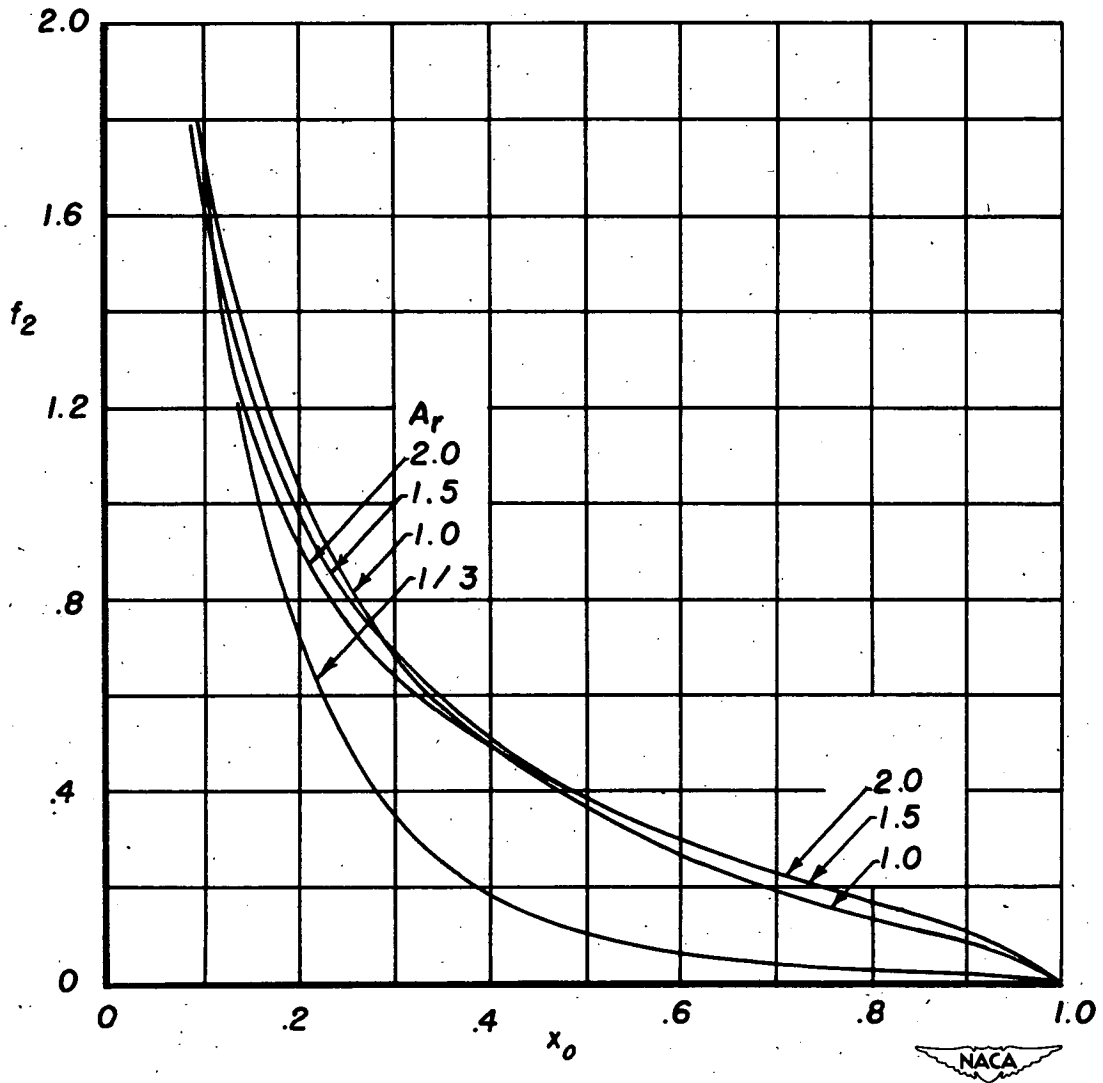
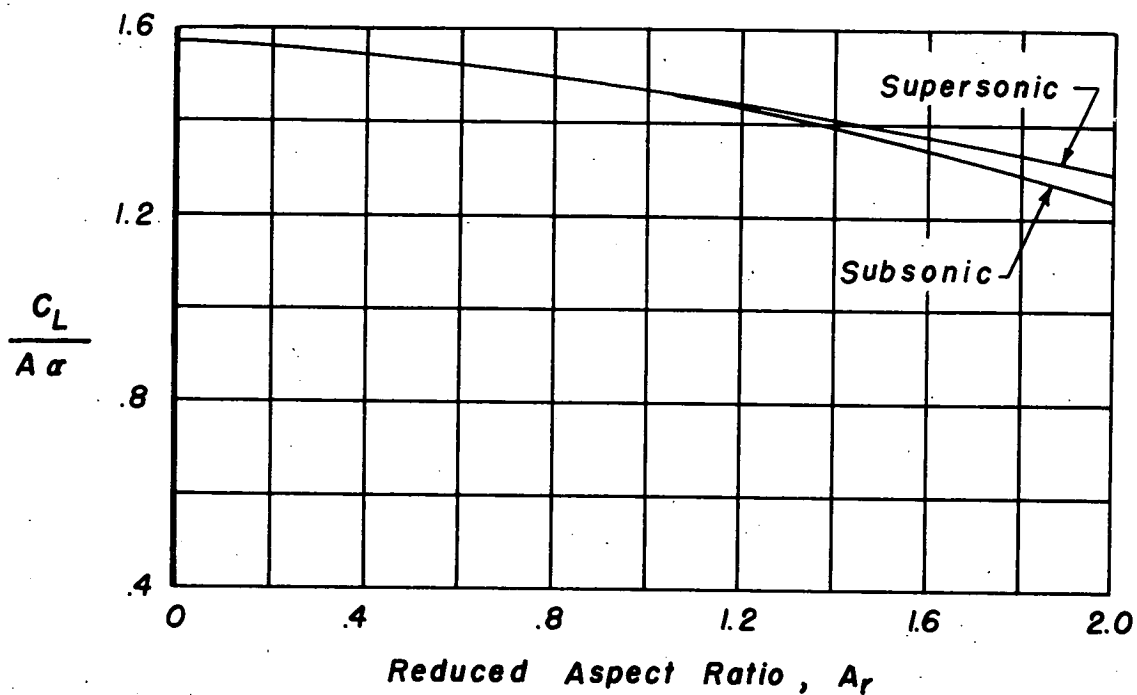
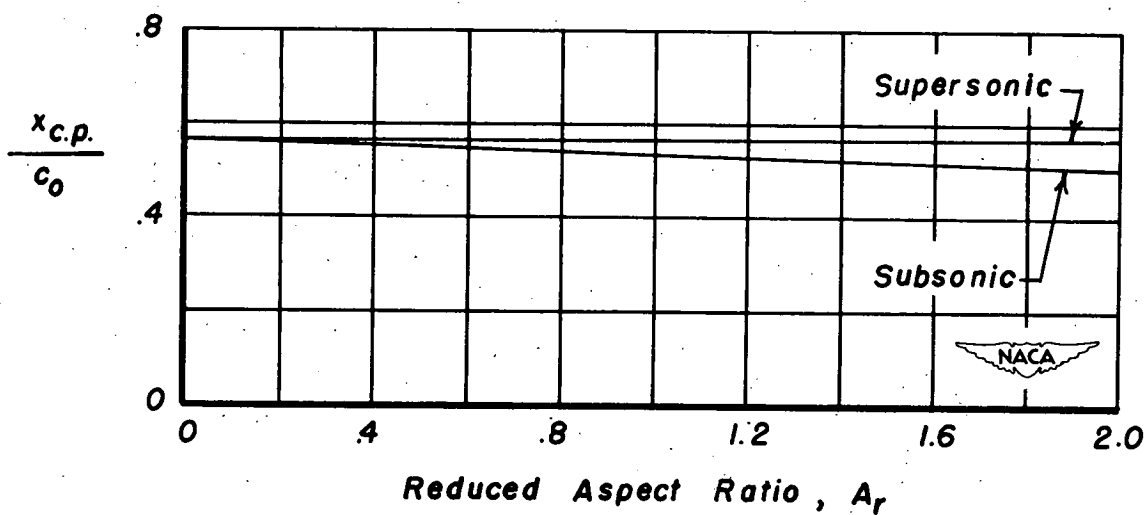


Figure 4.— Variation of chordwise correction factor f_2 for subsonic rectangular wing. $C_{L\alpha} = \frac{\pi A}{2} \int_0^1 f_2(x_0) dx_0$.



(a) Lift.



(b) Center of Pressure.

Figure 5.— Aerodynamic characteristics of a triangular wing having a low value of A_r .

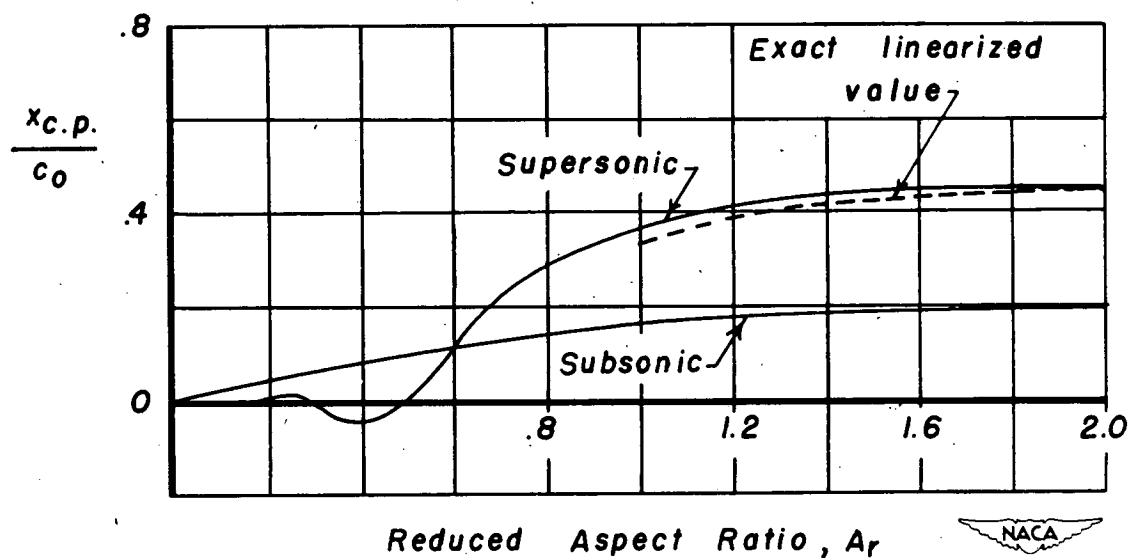
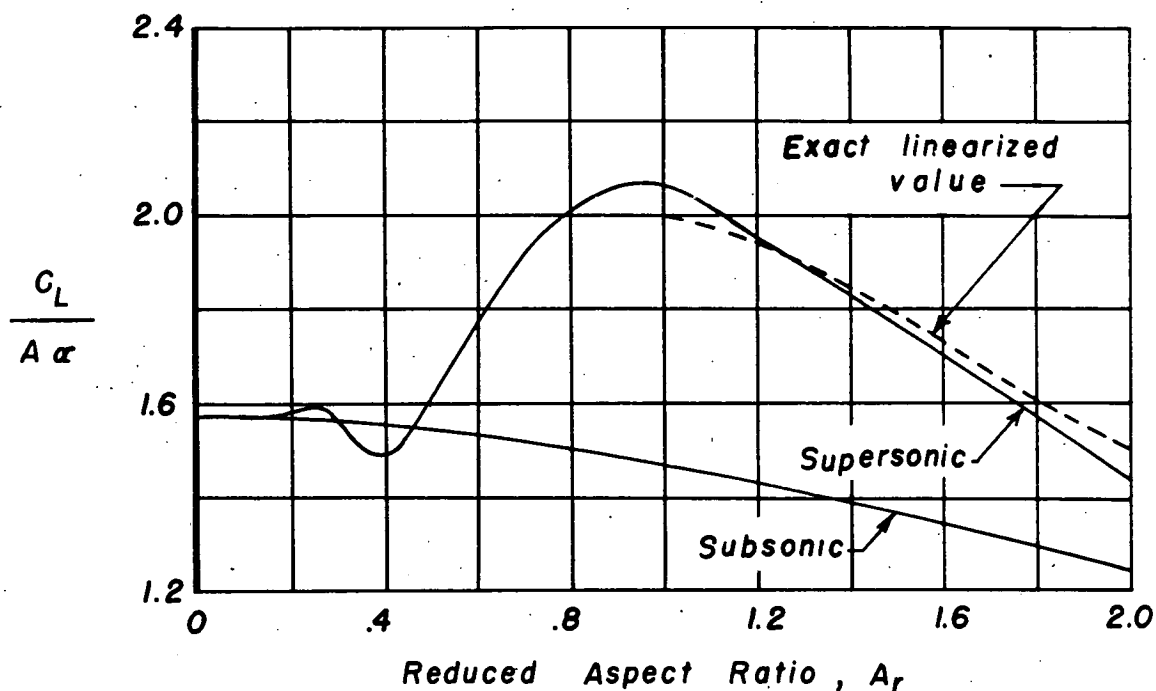


Figure 6.- Aerodynamic characteristics of rectangular wing having a low value of A_r .